IMA Journal of Numerical Analysis (2016) **36**, 80–107
doi:10.1093/imanum/dru064
Advance Access publication on February 3, 2015

Variational and linearly implicit integrators, with applications

Molei Tao*
School of Mathematics, Georgia Institute of Technology, Atlanta, GA, USA
*Corresponding author: mtao@gatech.edu

and

Houman Owhadi
Applied & Computational Mathematics, California Institute of Technology, Pasadena, CA, USA and Control & Dynamical Systems, California Institute of Technology, Pasadena, CA, USA

[Received on 16 January 2013; revised on 25 August 2014]

We show that symplectic and linearly implicit integrators proposed by Zhang & Skeel (1997, Cheap implicit symplectic integrators. *Appl. Numer. Math.*, **25**, 297–302) are variational linearizations of Newmark methods. When used in conjunction with penalty methods (i.e., methods that replace constraints by stiff potentials), these integrators permit coarse time-stepping of holonomically constrained mechanical systems and bypass the resolution of nonlinear systems. Although penalty methods are widely employed, an explicit link to Lagrange multiplier approaches appears to be lacking; such a link is now provided (in the context of two-scale flow convergence (Tao, M., Owhadi, H. & Marsden, J. E. (2010) Nonintrusive and structure-preserving multiscale integration of stiff ODEs, SDEs and Hamiltonian systems with hidden slow dynamics via flow averaging. *Multiscale Model. Simul.*, **8**, 1269–1324). The variational formulation also allows efficient simulations of mechanical systems on Lie groups.

Keywords: variational integrators; symplectic and linearly implicit; coarse time-stepping; constrained dynamics; mechanical system on Lie group.

1. Introduction and main results

Integrators: Symplectic integrators are popular for simulating mechanical systems due to their structure-preserving properties (e.g., Hairer *et al.*, 2006). Implicit methods, on the other hand, allow accurate coarse time-stepping of a class of stiff or multiscale problems (e.g., Li *et al.*, 2008; Filbet & Jin, 2010). It is also a classical treatment to linearize implicit methods so that expensive nonlinear solves can be avoided (e.g., Beam & Warming, 1976). Although linearizations of most implicit symplectic methods are not symplectic, Zhang and Skeel found a family of symplectic and linearly implicit integrators (Zhang & Skeel, 1997), which allows efficient and structure-preserving simulations. We show that their method is not only symplectic, but in fact variational.

Specifically, consider mechanical systems governed by Newton's equation:

$$\dot{x} = v, \quad M\dot{v} = -\nabla V(x), \tag{1.1}$$

where $V \in \mathcal{C}^2(\mathbb{R}^n)$ and M is an $n \times n$ symmetric, positive-definite constant matrix.

If we consider the following discrete Lagrangian (see Section 2.1 for explanations):

$$\begin{aligned}\tilde{\mathcal{L}}_d(x_k, x_{k+1}, a_k, a_{k+1}) = h\Bigg(&\frac{1}{2}\left(\frac{x_{k+1}-x_k}{h}\right)^{\mathrm{T}} M \left(\frac{x_{k+1}-x_k}{h}\right)\\ &-\frac{1}{2}\left(\beta h^2 \frac{1}{2} a_k^{\mathrm{T}} M a_k + V(x_k) + \beta h^2 a_k^{\mathrm{T}} \nabla V(x_k) + \frac{1}{2}\beta^2 h^4 a_k^{\mathrm{T}} \operatorname{Hess} V(x_k) a_k\right)\\ &-\frac{1}{2}\Bigg(\beta h^2 \frac{1}{2} a_{k+1}^{\mathrm{T}} M a_{k+1} + V(x_{k+1}) + \beta h^2 a_{k+1}^{\mathrm{T}} \nabla V(x_{k+1})\\ &+\frac{1}{2}\beta^2 h^4 a_{k+1}^{\mathrm{T}} \operatorname{Hess} V(x_{k+1}) a_{k+1}\Bigg)\Bigg),\end{aligned} \tag{1.2}$$

then the Euler–Lagrange equation of the variational principle

$$\delta \sum_{k=1}^{N} \tilde{\mathcal{L}}_d(x_k, x_{k+1}, a_k, a_{k+1}) = 0$$

yields the following symplectic method (originally stated in Zhang & Skeel, 1997, Section 3).

INTEGRATOR 1.1 **Zhang and Skeel's symplectic method (Z&S)**:

$$\begin{cases} x_{k+1} = x_k + h v_k + \frac{1}{2} h^2 f_k, \\ v_{k+1} = v_k + \frac{1}{2} h (f_k + f_{k+1}), \\ a_k = -M^{-1} \nabla V(x_k) - M^{-1} \operatorname{Hess} V(x_k) \beta h^2 a_k, \\ f_k = a_k - \frac{1}{2} \beta^2 h^4 M^{-1} a_k \cdot V^{(3)}(x_k) \cdot a_k, \end{cases} \tag{1.3}$$

where $V^{(3)}(\cdot)$ is a third-order tensor corresponding to the third-derivative of V, the symbol $\cdot$ stands for tensor contraction and therefore $a_k \cdot V^{(3)}(x_k) \cdot a_k$ is again a vector.

For computational efficiency, a_k should be obtained by solving a symmetric linear system instead of inverting a matrix. In this sense, Z&S is linearly implicit.

THEOREM 1.2 Z&S is:

1. unconditionally linearly stable if $\beta \geqslant \frac{1}{4}$;
2. variational (and thus symplectic and conserving momentum maps);
3. second-order convergent (if stable) and can be made arbitrarily high-order convergent;
4. symmetric ('time-reversible').

Showing Z&S is variational ensures,[1] due to a discrete Noether theorem (e.g., Marsden & West, 2001; Hairer *et al.*, 2006), that it also preserves momentum maps that correspond to system symmetries. This additional preservation property is desired in mechanical system simulations. The variational formulation also leads to a possible extension to Lie groups (Section 4.5).

Constrained dynamics: One of our motivations for studying Z&S originates from a need for coarse time-steppings in penalty methods for constrained dynamics.

To model constrained dynamics, let

$$\mathcal{S}(q(t)) := \int_a^b \frac{1}{2}\dot{q}(t)^{\mathrm{T}} M \dot{q}(t) - V(q(t))\,\mathrm{d}t \tag{1.4}$$

be the action associated with system (1.1). Under a holonomic constraint $g(q) = 0$, the system evolution coincides with the critical trajectory on the constraint manifold, i.e., the solution of

$$\delta\mathcal{S}/\delta q = 0 \quad \text{and} \quad \text{for all } t,\ q(t) \in g^{-1}(0). \tag{1.5}$$

This trajectory can also be obtained by solving the differential algebraic system

$$\begin{cases} M\ddot{q} = -\nabla V(q) + \lambda^{\mathrm{T}} \nabla g(q), \\ g(q) = 0. \end{cases} \tag{1.6}$$

Penalty methods approximate rigid constraints by stiff potentials; this is a classical idea and we refer the reader to Rubin & Ungar (1957), Takens (1980), Terzopoulos *et al.* (1987) and Platt & Barr (1988) for a noncomprehensive list of references. More precisely, modify the potential energy $V(q)$ to $V(q) + \frac{1}{2}\omega^2 g(q)^{\mathrm{T}} g(q)$; then, the solution of (1.5) is approximated by the solution of the following unconstrained mechanical system:

$$M\ddot{q}^{\omega} = -\nabla V(q^{\omega}) - \omega^2 g(q^{\omega})^{\mathrm{T}} \nabla g(q^{\omega}), \tag{1.7}$$

where ω is large enough. Paraphrasing Platt & Barr (1988), the problem is, 'as a result of stiffness, the numerical differential equation solver takes very small time steps, using a large amount of computing time without getting much done'. Z&S alleviates this problem because it can use coarse time steps and does not solve nonlinear systems (see Section 1.2).

On a related matter, although penalty methods are widely employed and proved convergent to constrained dynamics (see Section 1.1), a quantitative analysis of its link to the Lagrange multiplier approach (1.6) appeared to be lacking. We show that the solution of (1.7) converges to that of (1.6) as $\omega \to \infty$ in the sense of two-scale flow convergence (see Tao *et al.*, 2010, Definition 1.1). More precisely, we have (explained in Section 3; throughout this paper, 'bounded' means having a norm bounded by an ω-independent constant) the following theorem.

THEOREM 1.3 Denote by $q^{\omega}(t)$ the solution to (1.7) with $q^{\omega}(0) = q_0$ and $\dot{q}^{\omega}(0) = \dot{q}_0$ (where $g(q_0) = 0$ and $(\mathrm{d}/\mathrm{d}t)g(q_0) = \nabla g(q_0) \cdot \dot{q}_0 = 0$). Suppose that M is nonsingular, $V(\cdot)$ is bounded from below, $V(q)$ diverges towards infinity as $|q| \to \infty$, $V(\cdot)$ and $g(\cdot)$ are C^2 with bounded derivatives, and for all

[1] In general, symplectic methods are only locally variational, but variational methods are symplectic; see, for instance, Marsden & West (2001).

$q \in g^{-1}(0)$, $\nabla g(q)$ has a constant rank equal to the codimension of the constraint manifold; then,

$$\lambda(t) := -\lim_{T\to 0}\lim_{\omega\to\infty}\frac{1}{T}\int_t^{t+T}\omega^2 g(q^\omega(s))\,\mathrm{d}s \tag{1.8}$$

exists. Also, the solution $q(t)$ of

$$\begin{cases} M\ddot{q}(t) = -\nabla V(q(t)) + \lambda(t)^{\mathrm{T}}\nabla g(q(t)), \\ g(q(t)) = 0, \quad q(0) = q_0, \quad \dot{q}(0) = \dot{q}_0 \end{cases} \tag{1.9}$$

exists and satisfies

$$q^\omega \xrightarrow{F} q \tag{1.10}$$

in the sense of two-scale flow convergence (Tao *et al.*, 2010), i.e., for all bounded $t \geqslant 0$ and all bounded and uniformly Lipschitz-continuous test function φ,

$$\lim_{T\to 0}\lim_{\omega\to\infty}\frac{1}{T}\int_t^{t+T}\varphi(q^\omega(s)) - \varphi(q(s))\,\mathrm{d}s = 0. \tag{1.11}$$

Outline of the paper: Section 2 derives Z&S from a variational principle, relates it to Newmark integrators and discusses its properties. Section 3 illustrates how penalty methods converge to the Lagrange multiplier approach. Section 4 applies the method to constrained systems (pendula and water molecular dynamics), a nonconstrained model of DNA division and a mechanical system on SO(3), illustrating the benefits of a variational formulation.

1.1 *On penalty methods*

The penalty strategy of replacing holonomic constraints by stiff potentials is widely used. For example, it is a common treatment in computer graphics (e.g., Terzopoulos *et al.*, 1987; Witkin *et al.*, 1987; Platt & Barr, 1988).

It is known that the penalized solution converges to constrained dynamics in C^1 topology, as long as its initial condition is in the tangent bundle of the constraint manifold. We refer the reader to, e.g., the pioneering work of Rubin & Ungar (1957) and Takens (1980), to Bornemann & Schütte (1997), Bornemann (1998) and Shatah & Zeng (2002) for recent progress, and to Hairer *et al.* (2006, Chapter XIV.3) for a review.

The reverse point of view has also been employed, particularly in molecular dynamics, where stiff oscillatory molecular bonds are replaced by rigid constraints for the purpose of allowing larger time-steps (e.g., Fixman, 1974; Schlick, 2010). If the initial velocity is not in the tangent plane, then a correction potential might also be required to account for the nonzero normal energy (e.g., Fixman, 1974; Reich, 1995; Schütte & Bornemann, 1997). The Fixman potential (Fixman, 1974) is a classical example of such a correction, in particular when investigating thermodynamic properties of molecular systems (see, e.g., Bajars *et al.*, 2011); on the other hand, Bornemann & Schütte (1995) suggest that Fixman might not be the right correction for deterministic systems.

1.2 *One constrained dynamics*

Other popular constrained dynamics methods include: generalized coordinates on the constraint manifold (e.g., Jain *et al.*, 1993) and Lagrange multipliers (e.g., SHAKE (Ryckaert *et al.*, 1977), RATTLE (Andersen, 1983), SETTLE (Hess *et al.*, 1997), LINCS (Miyamoto & Kollman, 1992) and M-SHAKE (Kräutler *et al.*, 2001)). The equivalence between these two approaches is well-established (e.g., Wendlandt & Marsden, 1997). These numerical methods allow an $o(1)$ integration step, but they also require solving nonlinear systems at each step. Unfortunately, linearization of these methods are no longer symplectic, and therefore resorting to linearization for a speed-up is at the risk of losing long-time accuracy.

The advantage of using a penalty approach depends on the system: if the system has a large number of coupled constraints, then an integration of the penalized system, even with small steps, would still be faster than generalized coordinate and Lagrange multiplier methods, which require solving high-dimensional nonlinear systems.

Z&S provides a compromise by allowing large integration steps ($o(1)$, independent of ω) with limited cost of a linear solve per iteration. It remains accurate when applied to penalized system (1.7), even though the $o(1)$ step does not resolve stiffness of the equation. This is because stiffness in this system results in fast oscillations nontangent to a stable slow manifold (Section 3). Although implicit methods damp high frequencies in oscillations (e.g., Hairer & Wanner, 1996), the approximation of fast oscillations by slower ones (as in Li *et al.*, 2008) is sufficient for the approximation of slow dynamics on the constraint manifold.

We refer the reader to M-SHAKE (Kräutler *et al.*, 2001) for an example of recent developments to the Lagrange multiplier method. While M-SHAKE is limited to systems with distance constraints, Z&S combined with the penalty method can implement arbitrary holonomic constraints.

2. Z&S: structure-preserving and stable integrators

2.1 *Derivation from Newmark integrators*

The Newmark family of algorithms are extensively used in structural dynamics (Newmark, 1959).

INTEGRATOR 2.1 **Newmark**:

$$\begin{cases} q_{k+1} = q_k + h\dot{q}_k + \dfrac{h^2}{2}[(1-2\beta)a_k + 2\beta a_{k+1}], \\ \dot{q}_{k+1} = \dot{q}_k + h[(1-\gamma)a_k + \gamma a_{k+1}], \\ a_k = -M^{-1}\nabla V(q_k). \end{cases} \tag{2.1}$$

Newmark is generally implicit when $\beta \neq 0$. When $\gamma = \frac{1}{2}$, it is second-order accurate and variational (Kane *et al.*, 2000), and we restrict ourselves to this case in this paper. Integrator 2.1 does not preserve the canonical symplectic form, and it was shown in Skeel *et al.* (1997) and Marsden & West (2001) that if one pushes forward the update map by a coordinate transform $\eta : TQ \to TQ$ defined as

$$(x, v) := \eta(q, \dot{q}) = \left(q + \beta h^2 M^{-1}\nabla V(q), \dot{q}\right), \tag{2.2}$$

then we obtain an integrator that preserves the canonical symplectic form on T^*Q.

INTEGRATOR 2.2 **Pushforward Newmark**:

$$\begin{cases} x_{k+1} = x_k + hv_k + \frac{1}{2}h^2 a_k, \\ v_{k+1} = v_k + \frac{1}{2}h(a_k + a_{k+1}), \\ a_k = -M^{-1}\nabla V(x_k + \beta h^2 a_k). \end{cases} \tag{2.3}$$

These two methods are unconditionally linearly stable if $\beta \geqslant \frac{1}{4}$ (Skeel *et al.*, 1997; Chiba & Kako, 2002). Newmark with $\beta \geqslant \frac{1}{4}$ is known to be nonlinearly stable under specific conditions (Hughes, 1977), and Pushforward Newmark is known to be stable near stable fixed points in nonresonant nonlinear settings (Skeel & Srinivas, 2000). Nevertheless, there are nonlinear cases in which Newmark is no longer stable (Kuhl & Ramm, 1996; Erlicher *et al.*, 2002). In fact, few convergent methods are unconditionally stable for arbitrary nonlinear systems to the authors' knowledge (see also Wood & Oduor, 1988).

Now, consider a second-order discretization of the action $\int_{kh}^{(k+1)h} L(x, \dot{x})\,\mathrm{d}t$, where $L = \frac{1}{2}\dot{x}^{\mathrm{T}} M \dot{x} - V(x)$ is the Lagrangian for (1.1). This approximation, known as a discrete Lagrangian (see Marsden & West, 2001 for a review of variational integrators and Abraham & Marsden, 2008 for one of many excellent reviews of analytical mechanics), has the form

$$\begin{aligned} \mathcal{L}_d(x_k, x_{k+1}, a_k, a_{k+1}) = h \Bigg(& \frac{1}{2}\left(\frac{x_{k+1} - x_k}{h}\right)^{\mathrm{T}} M \left(\frac{x_{k+1} - x_k}{h}\right) \\ & - \frac{1}{2}\left(\beta h^2 \frac{1}{2} a_k^{\mathrm{T}} M a_k + V(x_k + \beta h^2 a_k)\right) \\ & - \frac{1}{2}\left(\beta h^2 \frac{1}{2} a_{k+1}^{\mathrm{T}} M a_{k+1} + V(x_{k+1} + \beta h^2 a_{k+1})\right)\Bigg). \end{aligned} \tag{2.4}$$

It can be shown that (2.3) is the Euler–Lagrange equation associated with (2.4), i.e., the equation that the critical point of the discretized action $\sum_k \mathcal{L}_d(x_k, x_{k+1}, a_k, a_{k+1})$ satisfies. Note that this variational formulation is explicit and distinct from the one implicitly defined in Marsden & West (2001). The novelty is the augmentation of acceleration parameters a_k s.

However, updates given by the Euler–Lagrange equation (2.3) are still implicit. Therefore, we Taylor-expand (2.4) to second order in a and derive (1.2). To obtain the corresponding discrete Euler–Lagrange equation, we compute $\partial \tilde{\mathcal{L}}_d / \partial a_k = 0$, which leads to

$$Ma_k + \nabla V(x_k) + \beta h^2 \operatorname{Hess} V(x_k) a_k = 0. \tag{2.5}$$

We then compute the discrete Legendre transform (see Marsden & West, 2001 for notation and terminology), which introduces the momentum and leads to

$$\begin{cases} p_k &= -D_1 L_d(x_k, x_{k+1}, a_k, a_{k+1}) \\ &= M\dfrac{x_{k+1} - x_k}{h} + \dfrac{h}{2}\left(-Ma_k + \dfrac{1}{2}\beta^2 h^4 a_k \cdot V^{(3)}(x_k) \cdot a_k\right), \\ p_{k+1} &= D_2 L_d(x_k, x_{k+1}, a_k, a_{k+1}) \\ &= M\dfrac{x_{k+1} - x_k}{h} - \dfrac{h}{2}\left(-Ma_{k+1} + \dfrac{1}{2}\beta^2 h^4 a_{k+1} \cdot V^{(3)}(x_{k+1}) \cdot a_{k+1}\right). \end{cases} \tag{2.6}$$

Since the velocity and momentum are related via $v_k = M^{-1} p_k$, we obtain the Z&S update (1.3).

Because the new discrete Lagrangian $\tilde{\mathcal{L}}_d$ is quadratic in a, nonlinear solves in Pushforward Newmark are replaced by linear solves in Z&S. Consequently, Z&S exhibits a speed advantage. Numerical illustrations of this advantage are in Section 4.

2.2 *On Z&S*

Linearizing equations: Z&S is obtained as the linearization of a Pushforward Newmark update map combined with a small correction. More precisely, the Taylor expansion of Line 3 of (2.3) leads to (2.5), and Lines 1 and 2 in (2.3) can be rewritten in terms of momentum as

$$\begin{cases} p_k & = -D_1 L_d(x_k, x_{k+1}, a_k, a_{k+1}) \\ & = M\dfrac{x_{k+1}-x_k}{h} + \dfrac{h}{2}(-Ma_k), \\ p_{k+1} & = D_2 L_d(x_k, x_{k+1}, a_k, a_{k+1}) \\ & = M\dfrac{x_{k+1}-x_k}{h} - \dfrac{h}{2}(-Ma_{k+1}). \end{cases}$$

The differences are two $\mathcal{O}(h^5)$ terms (corresponding to $\frac{1}{4}\beta^2 h^5 a \cdot V^{(3)}(x) \cdot a$). To be consistent with the literature, we summarize this variant using velocity instead of momentum as follows.

INTEGRATOR 2.3 **Zhang and Skeel's method simplified (Z&Ss)**:

$$\begin{cases} x_{k+1} = x_k + hv_k + \frac{1}{2}h^2 a_k, \\ v_{k+1} = v_k + \frac{1}{2}h(a_k + a_{k+1}), \\ a_k = -(M + \operatorname{Hess} V(x_k)\beta h^2)^{-1}\nabla V(x_k). \end{cases} \tag{2.7}$$

THEOREM 2.4 Z&Ss is:

1. unconditionally linearly stable if $\beta \geqslant \frac{1}{4}$;
2. symplectic if the $n \times n$ matrix $M + \operatorname{Hess} V(x)\beta h^2$ commutes with the $n \times n$ matrix $V^{(3)}(x) \cdot (M + \operatorname{Hess} V(x)\beta h^2)^{-1} \cdot \nabla V(x)$ ($\cdot$ is tensor contraction);
3. second-order convergent (if stable) and can be made arbitrarily high-order convergent;
4. symmetric ('time-reversible').

Z&Ss is not always symplectic due to the removal of $\mathcal{O}(h^5)$ terms. However, it requires no high-order tensor operations, and is thus a good choice for high-dimensional problems.

Partial Newton solve: Line 3 of Z&Ss can be viewed as executing only the first step of a Newton solver for the nonlinear equation $a_k = -M^{-1}\nabla V(x_k + \beta h^2 a_k)$.

Preconditioning, filtering and regularization: The factor of $(M + \operatorname{Hess} V(x)\beta h^2)^{-1}$ in front of $\nabla V(x)$ can be thought of as an optimization preconditioner or a way to filter (Hesthaven *et al.*, 2007; Faou & Grebert, 2011)/regularize (García-Archilla *et al.*, 1999; Sanz-Serna, 2008) high-frequency oscillations.

2.3 *Properties*

(Proofs of results introduced in this paragraph are standard and available online at http://www.math.gatech.edu/∼mtao/TaOw14_supplemental.pdf [last accessed 18 January 2015])

THEOREM 2.5 (Stability) Z&S (Integrator 1.1) is unconditionally linearly stable if and only if $\beta \geqslant \frac{1}{4}$.

The proofs of the unconditional linear stability (for $\beta \geqslant \frac{1}{4}$) of Integrators 1.1 and 2.3 are similar. If the potential is of form $V(x) = V_0(x) + \epsilon^{-1} V_1(x)$, then the following modification of Z&Ss is unconditionally linearly stable[2] as long as $\beta > \frac{1}{4} + \mathcal{O}(\epsilon)$.

INTEGRATOR 2.6 **Simplified Z&Ss for stiff systems** ($\epsilon^{-1} \gg 1$):

$$\begin{cases} x_{k+1} = x_k + h v_k + \frac{1}{2} h^2 a_k, \\ v_{k+1} = v_k + \frac{1}{2} h (a_k + a_{k+1}), \\ a_k = -M^{-1} (\nabla V_0(x_k) + \epsilon^{-1} \nabla V_1(x_k)) - M^{-1} \epsilon^{-1} \operatorname{Hess} V_1(x_k) \beta h^2 a_k. \end{cases} \tag{2.8}$$

THEOREM 2.7 (Consistency) Consider an integrator for (1.1) given by

$$\begin{cases} x_{k+1} = x_k + h v_k + \frac{1}{2} h^2 a_k, \\ v_{k+1} = v_k + \frac{1}{2} h (a_k + a_{k+1} + h^4 g(x_k) + h^4 g(x_{k+1})), \\ a_k = -M^{-1} \nabla V(x_k) - M^{-1} f(x_k) h^2 a_k, \end{cases} \tag{2.9}$$

where $f, g \in \mathcal{C}(Q)$ are arbitrary functions. If $V \in \mathcal{C}^3(Q)$, this integrator has third-order truncation error.

COROLLARY 2.8 Z&S (Integrator 1.1), Z&Ss (Integrator 2.3) and simplified Z&Ss for stiff systems (Integrator 2.6) are second-order convergent, provided that they are stable.

Symmetry (i.e., time-reversibility) is one desired property of numerical integrators, because it leads to good long-time performance (see, for instance, Hairer *et al.*, 2006 or Leimkuhler & Reich, 2004).

THEOREM 2.9 (Symmetry/time-reversibility) Let $f \in \mathcal{C}^1(Q)$ be an arbitrary function. The integrator defined by

$$\begin{cases} x_{k+1} = x_k + h v_k + \frac{1}{2} h^2 f_k, \\ v_{k+1} = v_k + \frac{1}{2} h (f_k + f_{k+1}), \\ f_k = f(x_k) \end{cases} \tag{2.10}$$

is symmetric (time-reversible).

COROLLARY 2.10 Z&S (Integrator 1.1) is symmetric (time-reversible).

REMARK 2.11 Arbitrary high-order Z&S can be obtained using standard splitting schemes as in Neri (1988), Yoshida (1990) and Hairer *et al.* (2006). A fourth-order example is provided in Supplementary Material.

[2] In the sense that the solution remains bounded for all h when V_0 has Lipschitz-continuous first-derivative with bounded Lipschitz constant and V_1 is quadratic and positive definite.

THEOREM 2.12 Z&S (Integrator 1.1) is symplectic.

LEMMA 2.13 (Symplecticity) Consider an integrator given by (2.10). If $f \in \mathcal{C}^1(Q)$ is a function with symmetric Jacobian, then this integrator is symplectic.

REMARK 2.14 The commutation condition in Theorem 2.4 ensures a symmetric Jacobian, and hence the symplecticity of Z&Ss. Two very special cases where this condition is satisfied are: when the system contains only 1 degree of freedom, or when Hess(V) can be diagonalized by a matrix independent of x.

REMARK 2.15 Fully nonlinear implicit symplectic methods (e.g., midpoint or Newmark) are not exactly symplectic due to numerical errors in nonlinear solves, which are often much larger than those in linear solves.

3. Lagrange multiplier methods as limits of penalty methods

Lagrange multiplier and penalty methods, respectively, simulate (1.6) and (1.7). It is known (Sections 1.1 and 1.2) that both are equivalent to constrained dynamics (1.5) (the latter in the $\omega \to \infty$ limit). We now quantify the equivalence between the two.

First, observe that this equivalence is *not* necessarily achieved via

$$\lambda(t) = -\lim_{\omega\to\infty} \omega^2 g(q^\omega(t)). \tag{3.1}$$

Consider, for instance, a 2 degrees of freedom example, in which $V(q) = (q_2 - q_1)^2/2$, $g(q) = q_1$, $q(0) = [0; 1]$ and $p(0) = [0; 0]$. Lagrange multiplier method (1.6) yields $q_1(t) = 0$, $q_2(t) = \cos t$ and $\lambda(t) = -\cos t$. Penalty method (1.7) leads to $q_1^\omega(t) = (1/\sqrt{4+\omega^4})(\cos(\omega_1 t) - \cos(\omega_2 t))$, where $\omega_{1,2} = \sqrt{(2+\omega^2 \mp \sqrt{4+\omega^4})/2}$. We see (3.1) cannot hold because $\lim_{\omega\to\infty} \omega^2 q_1^\omega(t)$ does not exist due to fast oscillations.

The appropriate notion of equivalence is provided by Theorem 1.3. The idea is as follows: energy conservation implies that $g(q^\omega)$ is at most $\mathcal{O}(1/\omega)$ (see Lemma A.1). In fact, $g(q^\omega)$ can be further shown to be $\mathcal{O}(1/\omega^2)$ (see Remark A.3 or Kevorkian & Cole, 1996), and constraints are satisfied with small errors that oscillate rapidly. To describe the Lagrange multiplier system (1.6) as a limit of penalized systems (1.7), the convergence of these fast oscillations should be understood in a weak sense, whereas slow dynamics on the constrained manifold converges strongly. Thus, we employ two-scale flow convergence (Equation (1.11)) for this description. Convergence is first proved for a flat constraint manifold (Lemma A.2), and then local charts are patched together (see appendix); this leads to Theorem 1.3.

REMARK 3.1 If the limit in (3.1) exists, then (1.8) simplifies to (3.1) and two-scale F-convergence becomes strong convergence.

4. Application examples

Z&S (Integrator 1.1) is applied in Sections 4.1, 4.2 and 4.4; Section 4.3 employs simplified Z&Ss for a stiff system (Integrator 2.6) due to its efficiency for high-dimensional systems; Section 4.5 is based on variational formulation (1.2).

Speed comparisons are provided in terms of running times (using Matlab 7.7 on an Intel Core 2 Duo 2.4G laptop, with nonlinear solver of 'fsolve'); however, these numbers are machine and platform dependent (e.g., Matlab is very well optimized for linear algebra), and should serve only as a qualitative illustration of efficiencies.

4.1 *Double pendulum*

Implementation: One way to represent planar double pendulum is to use 4 degrees of freedom and 2 nonlinear constraints. Using the notation of (1.7), we have

$$M = \begin{bmatrix} m_1 & 0 & 0 & 0 \\ 0 & m_1 & 0 & 0 \\ 0 & 0 & m_2 & 0 \\ 0 & 0 & 0 & m_2 \end{bmatrix}, \quad \begin{aligned} V(x_1, y_1, x_2, y_2) &= -\mathrm{g}y_1 - \mathrm{g}y_2, \\ g(x_1, y_1, x_2, y_2) &= \begin{bmatrix} x_1^2 + y_1^2 - L_1^2 \\ (x_2 - x_1)^2 + (y_2 - y_1)^2 - L_2^2 \end{bmatrix}. \end{aligned}$$

For simplicity, we adopt a dimensionless convention and assume $m_1 = m_2 = \mathrm{g} = 1$.

The Z&S simulation of the penalized system (1.7) is straightforward. SHAKE (Ryckaert *et al.*, 1977) is used as the Lagrangian multiplier method in our experiments; it is nonlinearly implicit.

Symplectic integration in generalized coordinates θ, ϕ ($x_1 = L_1 \sin\theta$, $y_1 = -L_1 \cos\theta$, $x_2 = L_1 \sin\theta + L_2 \sin\phi$, $y_2 = -L_1 \cos\theta - L_2 \cos\phi$) is also implicit. This is because, after writing down the Lagrangian, one will note a position-dependent mass matrix of

$$\tilde{M}(\theta, \phi) = \begin{bmatrix} 2L_1^2 & L_1 L_2(\cos\theta \cos\phi + \sin\theta \sin\phi) \\ L_1 L_2(\cos\theta \cos\phi + \sin\theta \sin\phi) & L_2^2 \end{bmatrix}. \tag{4.1}$$

Consequently, even the most well-known 'explicit' variational integrators such as variational Euler (i.e., leapfrog) and velocity-Verlet, will be implicit.

Note that although g is quadratic, the penalized ODE is cubically nonlinear.

Results: Figure 1 illustrates errors of different methods. Newmark (Integrator 2.1) with only the first step of nonlinear solve (Row 5) has a large error due to the loss of symplecticity, even though the method is still consistent. On the contrary, Z&S (Row 6) yields small errors almost identical to those of fully nonlinearly solved Newmark (Row 4).

Z&S produces larger error than SHAKE, because there is modelling error due to finite ω in addition to integration error (Row 3). We chose an intermediate ω, which is sufficiently large to approximate the constraints, yet small enough to show that the penalized system is only an approximation. A larger ω leads to a more accurate approximation, but if it is too large, e.g., $\omega = 2000$ (i.e., a stiffness of $\omega^2 = 4 \times 10^6$), instability occurs in all Z&S, original Newmark and implicit midpoint due to strong nonlinearity.

If ω is finite, the approximation error is predicted to be $\mathcal{O}(\omega^{-2})$ (Remark A.3). See Fig. 2(a) for a numerical illustration. Figure 2(b) compares the Lagrange multiplier computed by SHAKE with the one obtained from the penalized system via Theorem 1.3. There is no strong convergence, but only a two-scale F-convergence.

It is known that the double pendulum contains a chaotic region (e.g., Richter & Scholz, 1984). A variational integrator is desired for simulating such systems (Channell & Scovel, 1990; McLachlan & Atela, 1992). None of our symplectic simulations (Rows 1–4, 6) led to numerical leakage between regular and chaotic regions.

Generalized coordinate implicit VE (benchmark), SHAKE, variational Euler, Newmark with full nonlinear solve, Newmark with one-step nonlinear solve and Z&S, respectively, spent 91.3, 3.8, 1.0, 5.3, 0.2 (2.6 if Hess V is not analytically provided, but approximated by the nonlinear solver), and 0.4 s on the above simulation.

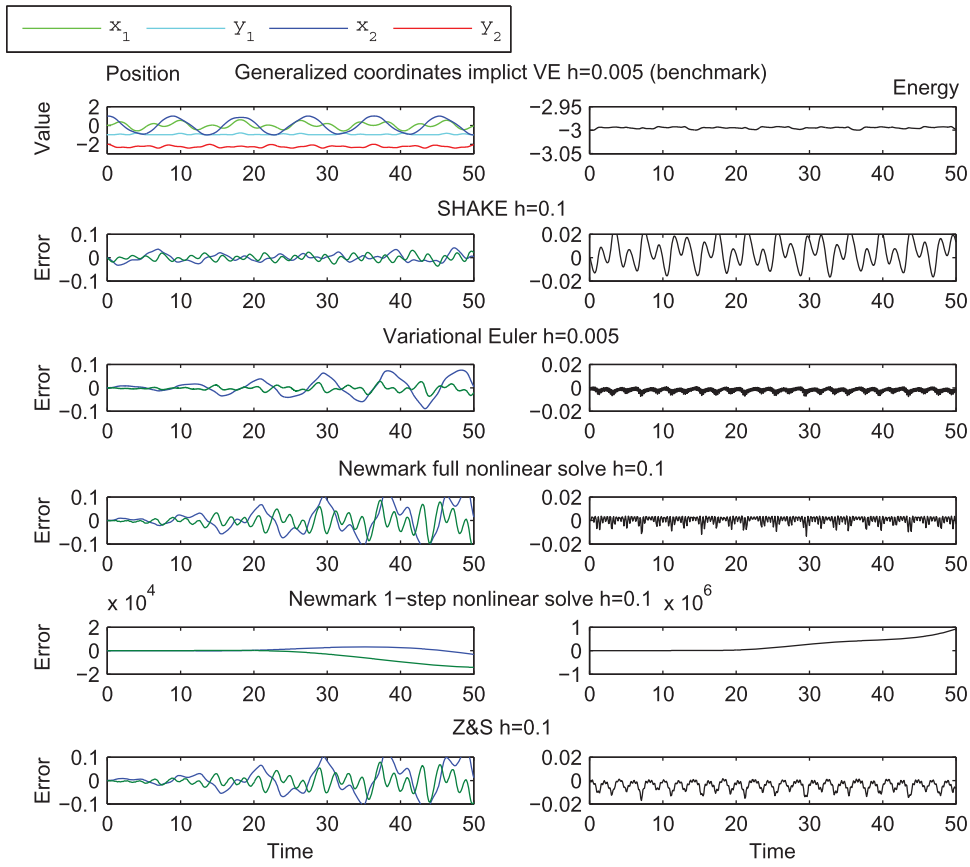

FIG. 1. Errors of SHAKE, variational Euler on the penalized system, Newmark (with nonlinear systems fully solved), linearly implicit Newmark (with only first iteration of nonlinear solve at each step), and Z&S. Benchmark is provided by small step variational Euler in generalized coordinates. Initial conditions are $x_1(0) = 0, y_1(0) = -1, x_2(0) = 1, y_2(0) = -2$, zero momenta; $L_1 = 1$ and $L_2 = \sqrt{2}$. $\omega = 20$ in Rows 3–6. $\beta = 0.4$. Row 3 uses $h = 0.1/\omega$ for stability, and Rows 2, 4–6 use a $20\times$ bigger $h = 0.1$. Position errors are only shown on x_2 and y_2 for readability.

4.2 *A simple high-dimensional example*: *a chain of many pendula*

Consider a chain of n pendula, which approximates a continuous rope. The system is similarly modelled by (1.7) with

$$M = \begin{bmatrix} 1 & 0 & \cdots & 0 & 0 \\ 0 & 1 & \cdots & 0 & 0 \\ \vdots & \vdots & \ddots & \vdots & \vdots \\ 0 & 0 & \cdots & 1 & 0 \\ 0 & 0 & \cdots & 0 & 1 \end{bmatrix}, \qquad V(x_1, y_1, \ldots, x_n, y_n) = -\sum_{i=1}^{n} y_i,$$

$$g(x_1, y_1, \ldots, x_n, y_n) = \begin{bmatrix} x_1^2 + y_1^2 - L_1^2 \\ (x_2 - x_1)^2 + (y_2 - y_1)^2 - L_2^2 \\ \vdots \\ (x_n - x_{n-1})^2 + (y_n - y_{n-1})^2 - L_n^2 \end{bmatrix}.$$

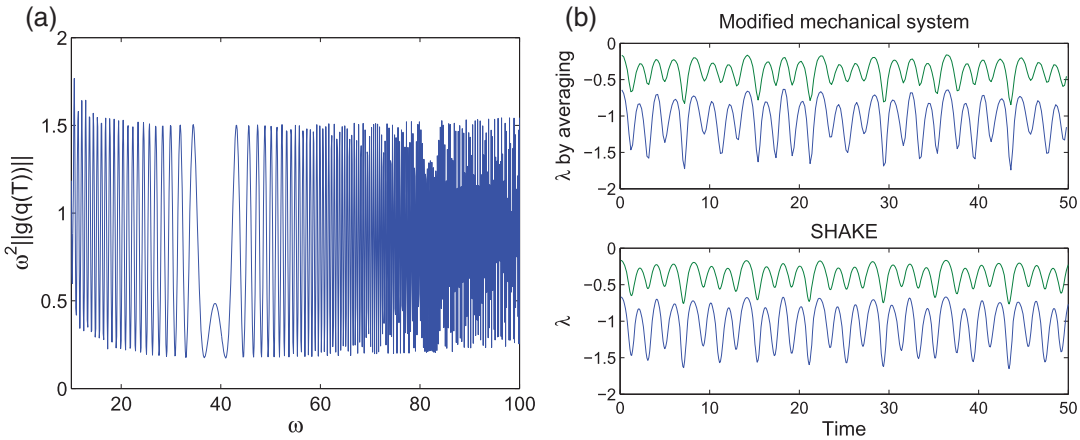

FIG. 2. Satisfaction of constraints and Lagrangian multiplier. Z&S with $h = 0.01$ is used (for smooth curve; Verlet would require $h = 0.001$ for stability); other parameters are the same as in Fig. 1. (a) $\omega^2\|g(q(T))\|$ numerically computed as a function of ω. $T = 50$ fixed; and (b) Lagrange multipliers computed by (1.8) from $\omega = 20$ penalized system and by SHAKE. The integral in (1.8) is approximated by empirical average over a time window of width 0.2.

Figure 3 shows good agreement between SHAKE and Z&S (trajectories instead of errors are shown due to lack of accurate benchmark—an analytical solution is unavailable, and Lagrange multiplier formulations and generalized coordinate approaches involve solving large nonlinear systems). SHAKE with $h = 0.025$, $h = 0.05$ and Z&S with $h = 0.05$, respectively, spent 16.5, 8.1 and 1.1 s in these simulations.

4.3 *Molecular dynamics of water cluster*

Consider the dynamics of water molecules, each interacting with others via nonbonded interactions of electrostatic and van der Waals forces (both highly nonlinear).

Water model: Use the popular TIP3P model (e.g., Jorgensen *et al.*, 1983). Let q_{ai} and p_{ai} be the position and momentum of the ath molecule's ith atom (both 3-vectors). The Hamiltonian is

$$\mathcal{H} = \sum_{a=1}^{N}\sum_{i=1}^{3}\frac{1}{2}p_{ai}^{\mathrm{T}}m_i^{-1}p_{ai} + \sum_{a=1}^{N-1}\sum_{b=a+1}^{N}\left(\sum_{i=1}^{3}\sum_{j=1}^{3}\frac{K_cQ_iQ_j}{r_{ai,bj}} + \frac{A}{r_{a2,b2}^{12}} - \frac{C}{r_{a2,b2}^{6}}\right), \tag{4.2}$$

where $r_{ai,bj} := \|q_{ai} - q_{bj}\|$ is the inter-atom distance, $m_1 = m_3$ are hydrogen mass and m_2 is oxygen mass, K_c is electrostatic constant, Q_i is the partial charge of atom i relative to the electron charge, and the A and C are Lennard–Jones constants that approximate van der Waals forces.

In this TIP3P model (or many other prevailing models such as SPC, BF, TIPS2 and TIP4P, which are discussed in, e.g., Jorgensen *et al.*, 1983; van der Spoel *et al.*, 1998), each water molecule is considered as a rigid body, with two O–H bond lengths and H–O–H bond angle fixed as constants r_{OH} and α_{HOH}. Detailed values of these model parameters could be found in, e.g., Jorgensen *et al.* (1983).

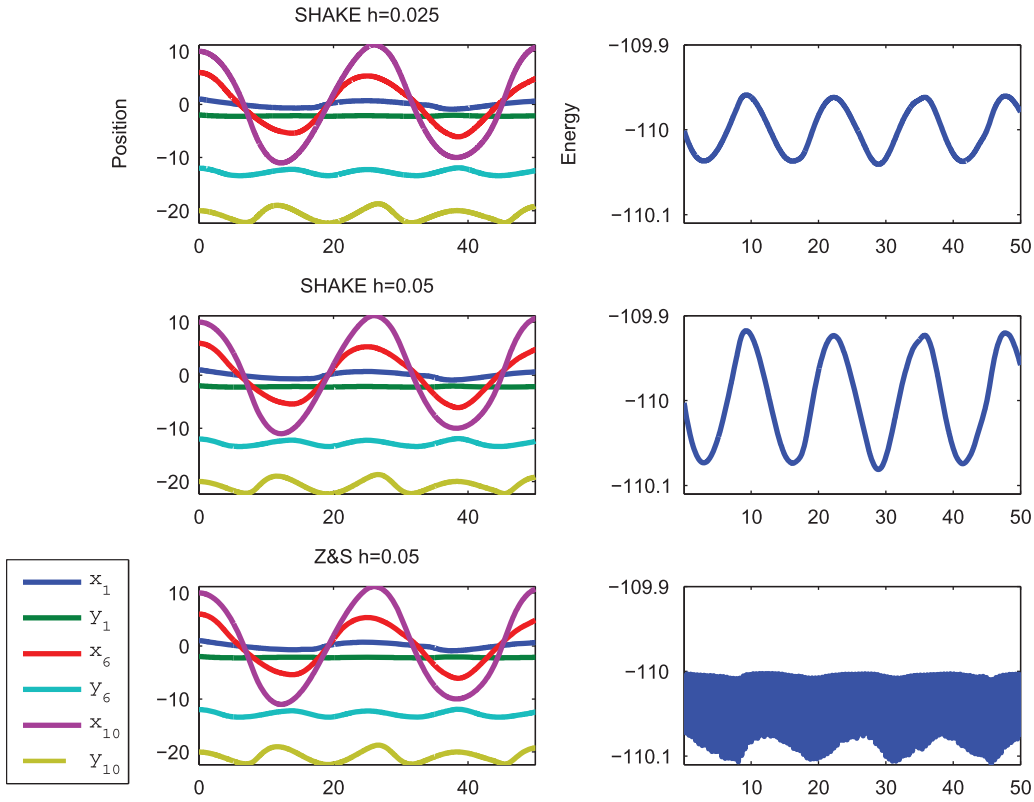

FIG. 3. Simulations by SHAKE with $h = 0.05$ and $h = 0.025$, and by Z&S with $h = 0.05$ on $\omega = 20$ penalized system. $n = 10$; $x_i(0) = i, y_i(0) = -2i$ for $i = 1, \ldots, n$ and initial momenta are zero; $L_i = \sqrt{5}$; $\beta = 0.4$. For clarity, not all degrees of freedom are shown.

Therefore, the following vectorial constraint enforces the geometry of molecules:

$$g(q) = \begin{bmatrix} (q_{11} - q_{12})(q_{11} - q_{12})^{\mathrm{T}} - r_{\mathrm{OH}}^2 \\ (q_{13} - q_{12})(q_{13} - q_{12})^{\mathrm{T}} - r_{\mathrm{OH}}^2 \\ (q_{11} - q_{13})(q_{11} - q_{13})^{\mathrm{T}} - r_{\mathrm{HH}}^2 \\ \vdots \\ (q_{N1} - q_{N2})(q_{N1} - q_{N2})^{\mathrm{T}} - r_{\mathrm{OH}}^2 \\ (q_{N3} - q_{N2})(q_{N3} - q_{N2})^{\mathrm{T}} - r_{\mathrm{OH}}^2 \\ (q_{N1} - q_{N3})(q_{N1} - q_{N3})^{\mathrm{T}} - r_{\mathrm{HH}}^2 \end{bmatrix}, \tag{4.3}$$

where $r_{\mathrm{HH}} := 2r_{\mathrm{OH}} \sin(\alpha_{\mathrm{HOH}}/2)$ is a constant. This leads to penalized Hamiltonian

$$\tilde{\mathcal{H}} = \mathcal{H} + \frac{1}{2}\omega^2 \sum_{a=1}^{N} \left(\left(r_{a1,a2}^2 - r_{\mathrm{OH}}^2\right)^2 + \left(r_{a3,a2}^2 - r_{\mathrm{OH}}^2\right)^2 + \left(r_{a1,a3}^2 - r_{\mathrm{HH}}^2\right)^2 \right). \tag{4.4}$$

Constant temperature simulation: Constant temperature simulations are of practical importance because (i) thermal fluctuations are an indispensable component of molecular dynamics; and (ii) the N-body system is chaotic and its long-time deterministic simulation has limited predictive power. We use Langevin dynamics (e.g., Schlick, 2010) as our constant temperature model.

In this model, molecules experience perturbation by noise and dissipation due to friction, and the dynamics can be expressed by the following SDEs:

$$\begin{cases} \mathrm{d}q = \dfrac{\partial \tilde{\mathcal{H}}}{\partial p}\,\mathrm{d}t, \\ \mathrm{d}p = -\dfrac{\partial \tilde{\mathcal{H}}}{\partial q}\,\mathrm{d}t - \gamma \dfrac{\partial \tilde{\mathcal{H}}}{\partial p}\,\mathrm{d}t + \sqrt{2\gamma\beta^{-1}}\,\mathrm{d}W, \end{cases} \tag{4.5}$$

where W is a $9N$-dimensional Wiener process, $\beta^{-1} > 0$ is the constant temperature and $\gamma > 0$ is dissipation strength. The system admits an invariant measure of Boltzmann–Gibbs (BG; also known as the canonical ensemble), given by

$$\pi(q,p) = Z^{-1} \exp(-\beta \tilde{\mathcal{H}}), \tag{4.6}$$

where $Z = \int_{\mathbb{R}^{18N}} \exp(-\beta\tilde{\mathcal{H}})\,\mathrm{d}q\,\mathrm{d}p$ is the partition function.

To simulate (4.5), we use the Geometric Langevin Algorithm (GLA; see Bou-Rabee & Owhadi, 2010). GLA allows for an extension of Hamiltonian integrators to Langevin integrators. It is a splitting scheme, based on composing the one-step update of a deterministic integrator with the exact flow of an Ornstein–Uhlenbeck process (given by $\mathrm{d}p = -\gamma M^{-1} p\,\mathrm{d}t + \sqrt{2\gamma\beta^{-1}}\,\mathrm{d}W$, i.e., driftless noise and friction). It has been shown (Bou-Rabee & Owhadi, 2010) that if the deterministic integrator is symplectic, then GLA not only provides a good approximation of trajectories, but also of BG (the invariant distribution). In this example, the deterministic building block is simplified Z&Ss (Integrator 2.6) or SHAKE.

Constant temperature molecular dynamics is a rich research field, and our investigation will only be numerical. The thermodynamic properties of a system with strong restraint may not be equivalent to those of a constrained system (e.g., Bajars *et al.*, 2011); the Fixman potential is a classical way to correct the difference (see Perchak *et al.*, 1985 for a debate on the validity of this correction). Proving that a numerical method samples a good approximation of the invariant distribution is nontrivial. Bou-Rabee & Owhadi (2010) combine ergodicity with the backward error analysis of symplectic integrators to show that the invariant distribution is preserved with a high order of accuracy. It is conjectured (Bou-Rabee & Owhadi, 2010, Remark 2.1) that SHAKE + GLA approximately samples a constrained BG distribution

$$\hat{\pi}(q,p) = \hat{Z}^{-1} \exp(-\beta \mathcal{H}), \tag{4.7}$$

where $\hat{Z} = \int_{T^*g^{-1}(0)} \exp(-\beta\mathcal{H})\,\mathrm{d}q\,\mathrm{d}p$. Relating (4.6) and (4.7) is left as a future investigation. See Vanden-Eijnden & Ciccotti (2006), Bajars *et al.* (2011), Hartmann (2008) and Lelièvre *et al.* (2012) for more about finite temperature constrained dynamics.

Numerical results: One quantity of interest in a water cluster is the distribution of interatomic oxygen–oxygen distances in the thermal equilibrium limit, also known as the OO radial distribution (Jorgensen *et al.*, 1983). To illustrate the accuracy of Z&S in sampling BG, Fig. 4 shows histograms obtained by long-time simulations of SHAKE and simplified Z&Ss (Integrator (2.6)) that approximate this distribution. We chose a system of size $N = 7$ (i.e., 63 degrees of freedom) so that peaks in the distribution could be clearly distinguished. SHAKE required 13472 s, including 12284 s on nonlinear

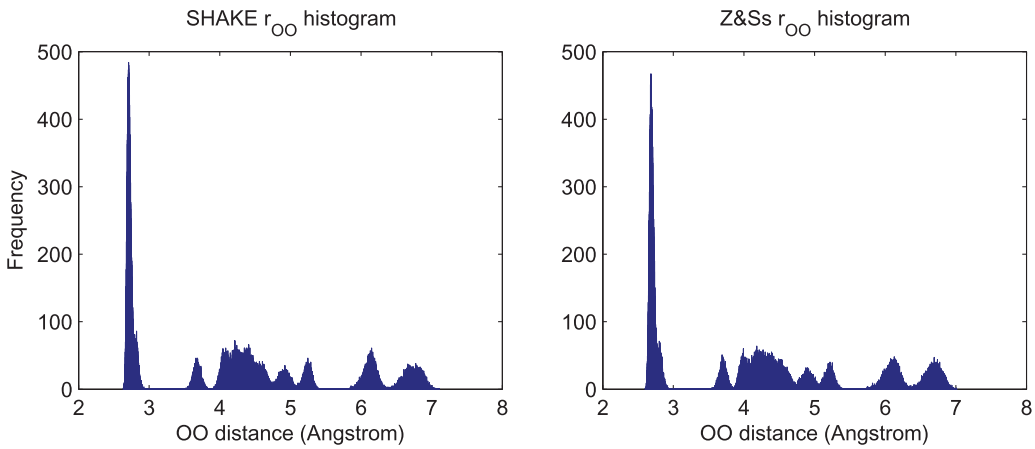

FIG. 4. Empirical OO radial distribution in a 7-water cluster obtained by long-time ($T = 10000$) simulations of SHAKE and simplified Z&Ss.

solves (with tolerances of 10^{-6} on variable and 10^{-10} on function value), whereas simplified Z&Ss used 1549 s, including 67 s on linear solves. Parameters are $\omega = 20$, $h = 0.05$ in both simulations, $\gamma = 0.01$ and $\beta = 50$.

We also provide two deterministic simulations (with noise and friction turned off; other parameters remain unchanged unless indicated otherwise): (i) Fig. 5 compares Lagrange multipliers computed by SHAKE and from the penalized system to illustrate Theorem 1.3. (ii) Figure 6 compares simplified Z&Ss, SHAKE and partially solved Newmark (nonsymplectic) in terms of energy and momentum conservations. Simplified Z&Ss lost symplecticity due to simplification, but it still exhibits improved preservation properties comparing with partially solved Newmark.

To test scalability, we increase N to 100 (900 degrees of freedom) and illustrate results in Fig. 7. SHAKE spent 42234 s, including 14272 s on solving nonlinear systems and ~ 28000 s on computing V and ∇V, whereas simplified Z&Ss spent 30059 s, including 319 s on solving linear systems, and ~ 29000 s on V, ∇V and Hess V.

Efficiency of force evaluation: Although simplified Z&Ss accelerates updates by linearization, for large systems the computational bottleneck is likely to be on force evaluations, but not updates. Fortunately, significant progress has been made to accelerate force evaluations, such as the fast multipole method (Greengard & Rokhlin, 1987), or simply the idea of ignoring weak long-range forces. We did not employ any of them, but they can be used in adjunct to simplified Z&Ss.

Times spent on force evaluations by SHAKE and simplified Z&Ss are comparable; Hessian computations in simplified Z&Ss did not incur much overhead. This is because the potential is a function of relative distances $r_{ij} = \|x_i - x_j\|$. For such f,

$$\frac{\partial^2 f(r)}{\partial x_i \partial x_j} = \frac{\partial r}{\partial x_i}\frac{\partial^2 f}{\partial r^2}\frac{\partial r}{\partial x_j} + \frac{\partial f}{\partial r}\frac{\partial^2 r}{\partial x_i \partial x_j}, \tag{4.8}$$

but $\partial r/\partial x$ and $\partial f/\partial r$ are already computed when calculating the gradient, $\partial^2 r/\partial x_i \partial x_j$ is cheap to obtain and $\partial^2 f/\partial r^2$ is the only new component of computation, but it is a scalar. In addition, nonlinear

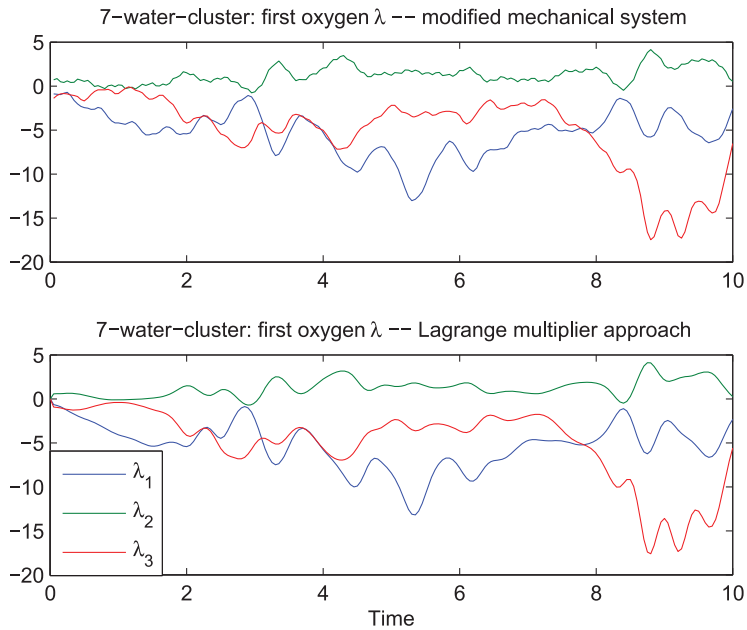

FIG. 5. Lagrange multipliers from the penalized system (simplified Z&Ss) and by SHAKE. Only the first oxygen atom is shown, and illustration is terminated before chaos. Empirical average uses a time window of width 0.2; ω is temporarily enlarged to 500 for clearer visualization of details.

solver (e.g., Newton) in Lagrange multiplier or generalized coordinate methods requires the Hessian too because the equation to be solved involves ∇V.

The linear system associated with the Hessian can also be solved in $\mathcal{O}(N)$ time. This is because the Hessian is dominated by a block diagonal due to localized stiff penalty terms in (4.4). Simplified Z&Ss further reduces the Hessian to completely block diagonal, and linear solves are executed molecule by molecule. Similar efficiency can be obtained for polymers as long as the number of bonds is at the same order as the number of atoms.

4.4 *Coarse time-stepping of a DNA model*

We now show how Z&S accelerates the simulation of an *unconstrained* multiscale system. Consider the simple DNA model proposed in Mezić (2006) and further studied, e.g., in Toit *et al.* (2009) and Koon *et al.* (2013). The displacement angle of the kth base in one strand, θ_k, follows:

$$\ddot{\theta}_k = \theta_{k+1} - 2\theta_k + \theta_{k-1} - \epsilon U'(\theta_k), \tag{4.9}$$

where $U(\theta) = (\exp(-a[1 - \cos(\theta) - x_0]) - 1)^2$ is a Morse potential modelling complementary base pairings between two DNA strands, and linear force models the tendency of alignment between neighbouring bases. Unitless parameters are $a = 7$, $x_0 = 0.3$, $\epsilon = \frac{1}{1400}$ and the number of base-pairs $N = 200$ (Toit *et al.*, 2009). Two stable configurations are given by minima of U and correspond to closed double strands. Nonlinearity in this system is critical, for it leads to transitions between meta-stable

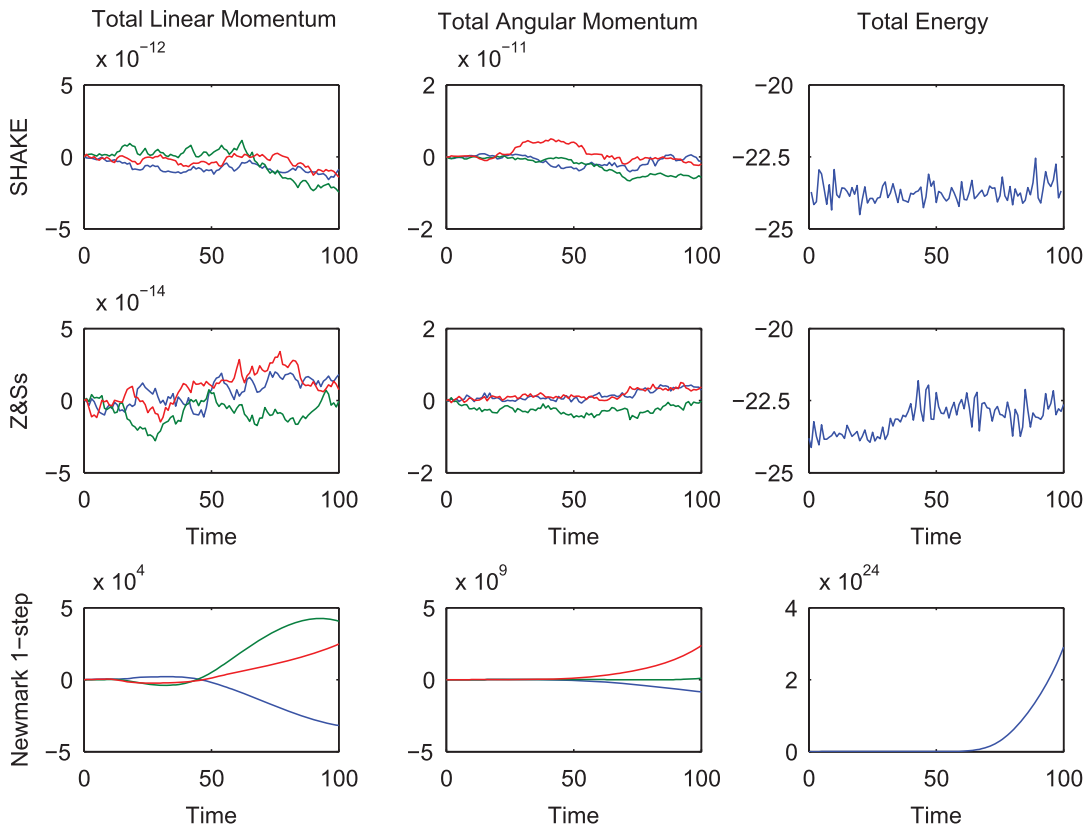

FIG. 6. Energy, linear and angular momentum preservation by simplified Z&Ss, SHAKE and partially solved Newmark. $h = 0.05$ for all. For clarity, plots are drawn with a 20:1 downsample rate.

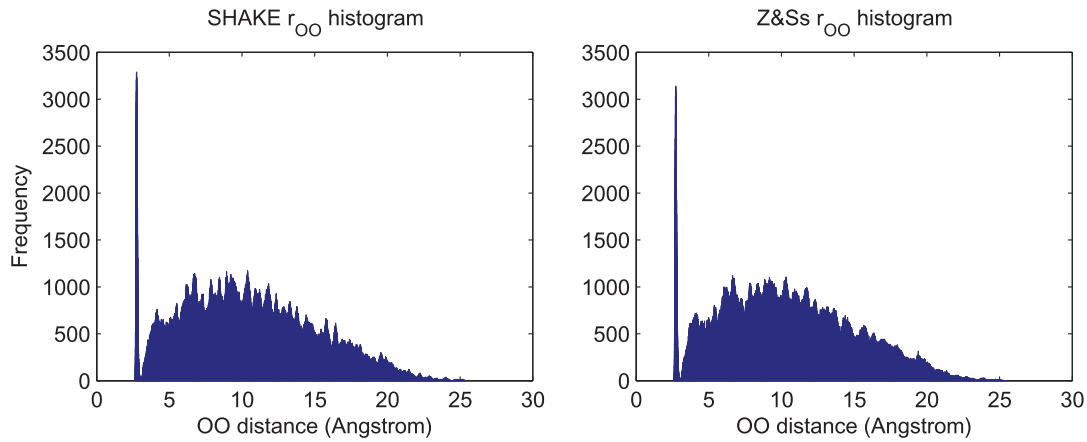

FIG. 7. Empirical OO radial distribution in a 100-water cluster obtained by simulations of SHAKE and simplified Z&Ss till $T = 1000$.

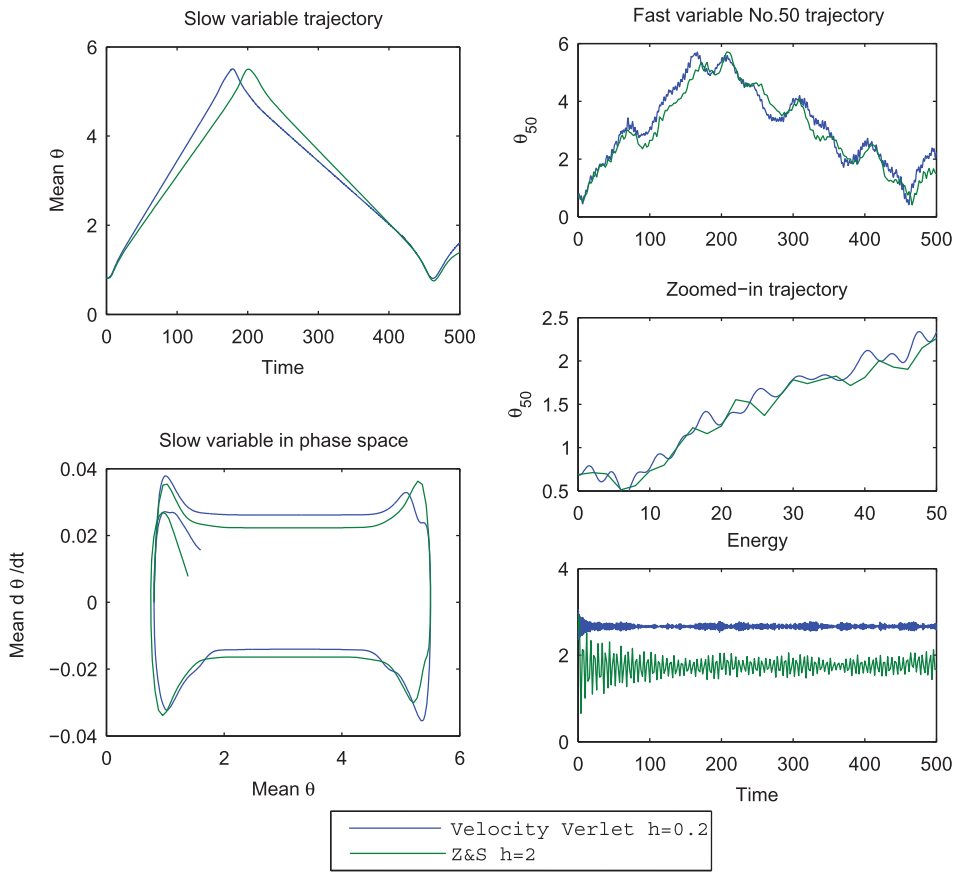

FIG. 8. DNA ($N = 200$ base-pairs) conformational transitions by Z&S and velocity-Verlet.

states that correspond to the opening of double strands. We simulate such transitions with initial positions $\theta_k = 0.8 + 0.1\xi_k$ (ξ_k i.i.d. standard norm), which is near a stable configuration, and initial momenta $\dot{\theta}_k = \cos(4\pi k/N)/\sqrt{N}$, which facilitates the opening-up of double strands (Toit *et al.*, 2009).

It is known Toit *et al.* (2009) that $\bar{\theta} = \sum \theta_k/N$ is a slow variable and can be used as a reaction parameter, whereas individual θ_k s are fast variables. Figure 8 presents simulations by velocity-Verlet (benchmark) and Z&S ($\beta = 0.3$) in these variables. The phase portrait shows that the DNA transits between meta-stable configurations $\theta = \arccos(0.7) \approx 0.795$ and $\theta = 2\pi - \arccos(0.7) \approx 5.49$. Note that these are long-time simulations and the system is chaotic (Mezić, 2006).

The Z&S energy is lower than the benchmark because fast oscillations are damped by large time-steps. Both $h = 0.2$ in velocity-Verlet and $h = 2$ in Z&S are near stability limits. The methods, respectively, used 23.26 and 3.24 s of CPU time.

4.5 *Lie group integration*

Formulating Z&S as a variational principle allows us to generalize the method to mechanical systems on Lie groups.

Consider a prototypical example of magnetized 3D rigid body with identity inertia matrix immersed in a constant magnetic field. The configuration space is $Q = \mathrm{SO}(3)$. Denote by $R(t) \in Q$ the (generalized) rigid body position; in coordinates it is a 3×3 matrix satisfying $R^{\mathrm{T}}R = I$. Suppose when $R = I$ both the magnetic field and the dipole are in the z-direction; then, the potential energy can be written as $V(R) = \langle \mu R e_3, B e_3 \rangle = B\mu e_3^{\mathrm{T}} R^{-1} e_3$, where B and μ are field strength and dipole moment, and $e_3 = [0\ 0\ 1]^{\mathrm{T}}$.

Let $\Omega(t) \in \mathbb{R}^3$ be convective angular velocity of the body; then the kinetic energy is $\frac{1}{2}\Omega^{\mathrm{T}}\Omega$. Introduce an isomorphism between $\mathbb{R}^3$ and $\mathfrak{so}(3)$ (the Lie algebra of $\mathrm{SO}(3)$) by

$$\Omega \mapsto \hat{\Omega} = \begin{bmatrix} 0 & -\Omega_3 & \Omega_2 \\ \Omega_3 & 0 & -\Omega_1 \\ -\Omega_2 & \Omega_1 & 0 \end{bmatrix}.$$

Then, $\dot{R} = R\hat{\Omega}$. It is known (Marsden & Ratiu, 2010) that dynamics of this mechanical system can be obtained from either of the following equivalent variational principles:

- $$\delta \int_0^T L(R, \dot{R})\, \mathrm{d}t = 0, \tag{4.10}$$

  with arbitrary variations of $R(t) \in Q$.

- $$\delta \int_0^T l(R, \xi)\, \mathrm{d}t = 0, \tag{4.11}$$

  with variations in the form $\delta\xi = \dot{\eta} + \mathrm{ad}_\xi \eta$ under $R \in Q$ and $\xi = R^{-1}\dot{R}$.

For our system, $L(R, \dot{R}) = \frac{1}{4}\mathrm{tr}(\dot{R}^{\mathrm{T}}\dot{R}) - B\mu e_3^{\mathrm{T}} R^{-1} e_3$ and $l(R, \hat{\Omega}) = \frac{1}{2}\Omega^{\mathrm{T}}\Omega - B\mu e_3^{\mathrm{T}} R^{-1} e_3$ (note $\Omega^{\mathrm{T}}\Omega = \frac{1}{2}\mathrm{tr}(\hat{\Omega}^{\mathrm{T}}\hat{\Omega})$).

We propose to simulate the system by modifying (4.10). The result is compared with a benchmark derived from (4.11) via the Hamilton–Pontryagin principle, backward Variational Euler discretization and Cayley approximation of the exponential map (see Iserles, 2001; Hairer *et al.*, 2006 for Cayley approximation, Bou-Rabee & Marsden, 2009 for the benchmark method and Iserles *et al.*, 2000; Lee *et al.*, 2007 for examples of other Lie group integrators). The benchmark uses update rules:

$$\begin{cases} R_{k+1} = R_k (I - h\hat{\Omega}_{k+1}/2)^{-1}(I + h\hat{\Omega}_{k+1}/2), \\ \hat{\Omega}_{k+1} = \hat{\Omega}_k + \dfrac{h^2}{4}\left(\hat{\Omega}_{k+1}^{\mathrm{T}}\hat{\Omega}_{k+1}\hat{\Omega}_{k+1}^{\mathrm{T}} - \hat{\Omega}_k^{\mathrm{T}}\hat{\Omega}_k\hat{\Omega}_k^{\mathrm{T}}\right) + hR_k \dfrac{\partial l}{\partial R}\left(R_k, \hat{\Omega}_{k+1}\right). \end{cases} \tag{4.12}$$

Note R is in a three-dimensional manifold, and the differential in the last term should not be computed as a partial derivative with respect to nine Cartesian coordinates of R; otherwise the last term will not be in $\mathfrak{so}(3)$. Instead, we follow Holm *et al.* (1998) and obtain

$$hR_k \frac{\partial l}{\partial R}(R_k, \hat{\Omega}_{k+1}) = hB\mu R_k \frac{-e_3^{\mathrm{T}} R_k^{-1} e_3}{\partial R_k} = hB\mu\left(\left(R_k^{-1} e_3\right) \times e_3\right)^{\wedge}. \tag{4.13}$$

Equation (4.12) is variational and thus numerically energy- and momentum preserving. Owing to Cayley approximation, it also preserves the SO(3) structure in the sense that $R_k^{\mathrm{T}} R_k = I$ up to arithmetic error.

However, variational methods of this type are intrinsically nonlinearly implicit due to curved geometry when Q is noncommutative (e.g., Bou-Rabee & Marsden, 2009; Kobilarov *et al.*, 2009).

Our goal is to avoid expensive nonlinear solves and bypass force evaluations that require geometric calculations (such as (4.13)). To do so, we first add penalization to (4.10):

$$\delta \int_0^T \frac{1}{4}\mathrm{tr}(\dot{R}^{\mathrm{T}}\dot{R}) - B\mu R(3,3) + \frac{1}{2}\omega^2 \mathrm{tr}\left((R^{\mathrm{T}}R - I)^{\mathrm{T}}(R^{\mathrm{T}}R - I)\right)\,\mathrm{d}t = 0,$$

where $R \in \mathrm{SO}(3)$ is relaxed to $R \in \mathbb{R}^{3\times 3}$. We then discretize the action as follows:

$$\begin{aligned}\mathcal{L}_d(R_k, R_{k+1}, a_k) = \mathrm{tr}&\left(\frac{1}{4}\left(\frac{R_{k+1}-R_k}{h}\right)^{\mathrm{T}}\left(\frac{R_{k+1}-R_k}{h}\right) - \beta h^2 \frac{1}{2}a_k^{\mathrm{T}}a_k\right)\\ &- B\mu e_3^{\mathrm{T}}\left(R_k + \beta h^2 a_k\right)e_3 - \mathrm{tr}\left(\frac{1}{2}\omega^2\left(\left(\left(R_k + \beta h^2 a_k\right)^{\mathrm{T}}\left(R_k + \beta h^2 a_k\right) - I\right)^2\right)\right).\end{aligned} \tag{4.14}$$

Finally, we truncate terms that are higher than second order in a_k. After using trace identities $\mathrm{tr}(AB) = \mathrm{tr}(BA)$ and $\mathrm{tr}(A^{\mathrm{T}}) = \mathrm{tr}(A)$, the truncated action simplifies to

$$\begin{aligned}\tilde{\mathcal{L}}_d(R_k, R_{k+1}, a_k) = \mathrm{tr}&\left(\frac{1}{4}\left(\frac{R_{k+1}-R_k}{h}\right)^{\mathrm{T}}\left(\frac{R_{k+1}-R_k}{h}\right) - \beta h^2 \frac{1}{2}a_k^{\mathrm{T}}a_k\right)\\ &- B\mu e_3^{\mathrm{T}}\left(R_k + \beta h^2 a_k\right)e_3 - \mathrm{tr}\left(\frac{1}{2}\omega^2\left(\left(R_k^{\mathrm{T}}R_k - I\right)^2 + 4\beta h^2\left(R_k^{\mathrm{T}}R_kR_k^{\mathrm{T}} - R_k^{\mathrm{T}}\right)a_k\right.\right.\\ &\left.\left. + 2\beta^2 h^4\left(a_k^{\mathrm{T}}a_kR_k^{\mathrm{T}}R_k + R_k^{\mathrm{T}}a_kR_k^{\mathrm{T}}a_k + a_k^{\mathrm{T}}R_kR_k^{\mathrm{T}}a_k - a_k^{\mathrm{T}}a_k\right)\right)\right).\end{aligned}$$

Unconstrained variation of this action with respect to a_k gives

$$a_k = -B\mu e_3 e_3^{\mathrm{T}} - 2\omega^2(R_kR_k^{\mathrm{T}}R_k - R_k + \beta h^2(a_kR_k^{\mathrm{T}}R_k + R_ka_k^{\mathrm{T}}R_k + R_kR_k^{\mathrm{T}}a_k - a_k)). \tag{4.15}$$

Standard variational integrator construction leads to

$$p_k = -D_1\tilde{\mathcal{L}}_d(R_k, R_{k+1}, a_k), \quad p_{k+1} = D_2\tilde{\mathcal{L}}_d(R_k, R_{k+1}, a_k).$$

Let $f_k = a_k + 2\omega^2\beta^2h^4(a_k^{\mathrm{T}}a_kR_k^{\mathrm{T}} + a_k^{\mathrm{T}}R_ka_k^{\mathrm{T}} + R_k^{\mathrm{T}}a_ka_k^{\mathrm{T}})$ and use (4.15) for simplification; then the above becomes

$$\begin{cases} p_{k+1} = p_k + hf_k, \\ R_{k+1} = R_k + 2hp_{k+1}. \end{cases}$$

These are our variational linearized SO(3) integrators. Note that (4.14) is based on a first-order quadrature; the second-order trapezoidal rule would lead to

$$\begin{cases} p_{k+1/2} = p_k + \dfrac{h}{2}f_k, \\ R_{k+1} = R_k + 2hp_{k+1}, \\ p_{k+1} = p_k + \dfrac{h}{2}f_{k+1}. \end{cases}$$

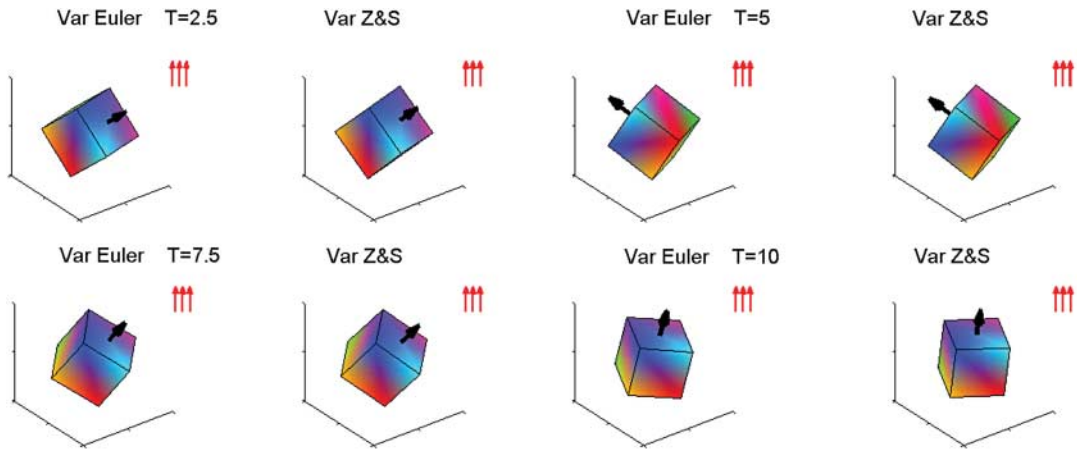

FIG. 9. Snapshots of magnetized rigid body dynamics. Red and black arrows represent magnetic field and dipole, respectively.

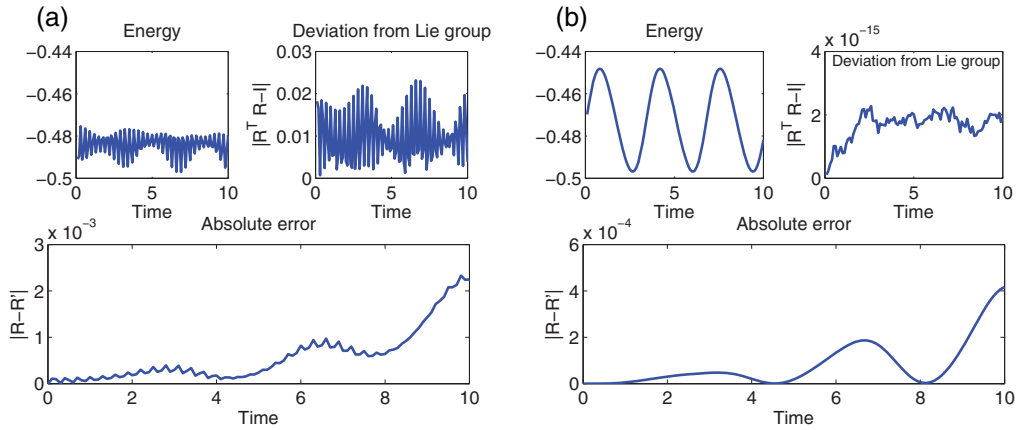

FIG. 10. Preservation of energy, Lie group structure and deviation from benchmark trajectory R'. (a) Variational Z&S ($h = 0.1$); and (b) variational Euler on Lie group ($h = 0.1$).

These are similar to Z&S updates (Integrator 1.1) although Z&S works in $\mathbb{R}^n$. Some may question the usefulness of a variational formulation, because one can represent R by a nine-dimensional vector, view the penalized system as Newton's equation and then use Z&S. In Z&S updates (1.3), however, $V^{(3)}$ is essentially a 6-tensor, and its brute-force calculation in coordinates, as well as its contractions with a from both left and right, will be unpleasant. A variational approach minimizes the involvement of coordinates and reduces the effort.

Figure 9 demonstrates benchmark ($h = 0.0001$) and variational Z&S simulations ($h = 0.1$, $\omega = 10$, $\beta = 0.4$); their difference, regarded as our method's error, is quantified in Fig. 10(a); the error of the benchmark method with $h = 0.1$ is also provided in Fig. 10(b) as a comparison. The full simulation is available at http://youtu.be/29deMRDRsuU (last accessed 18 January 2015). Initial conditions are $R(0) = I$ and $\Omega(0) = [1; 0.2; 0.1]$.

Our method and variational Euler with both $h = 0.1$, respectively, spent 0.03 and 1.45 s on computations. However, a variational Lie group integrator is much better at preserving the Lie group structure. Applicabilities of the two approaches are disjoint: for example, variational Z&S generally suits computer graphics better, where real time rendering requires high efficiency, while demand on accuracy is moderate (as long as the result looks good); to orient satellites (e.g., Junge & Ober-Bloebaum, 2005), on the other hand, one should choose variational Lie group integrators over variational Z&S, and it is worth CPU hours to precompute trajectories with high fidelity.

Acknowledgements

We thank Mathieu Desbrun for motivation and discussions, Joel Tropp and Eitan Grinspun for discussions, Carmen Sirois for proofreading the manuscript and anonymous reviewers for comments.

Funding

This work was supported by NSF grant CMMI-092600, a generous gift from UTRC and Courant Instructorship from New York University.

References

Abraham, R. & Marsden, J. E. (2008) *Foundations of Mechanics*, 2nd edn. Providence, RI: American Mathematical Society.

Andersen, H. C. (1983) Rattle: a 'velocity' version of the shake algorithm for molecular dynamics calculations. *J. Comput. Phys.*, **52**, 24–34.

Bajars, J., Frank, J. & Leimkuhler, B. (2011) Stochastic-dynamical thermostats for constraints and stiff restraints. *Eur. Phys. J. Spec. Top.*, **200**, 131–152.

Beam, R. M. & Warming, R. (1976) An implicit finite-difference algorithm for hyperbolic systems in conservation-law form. *J. Comput. Phys.*, **22**, 87–110.

Bornemann, F. (1998) *Homogenization in Time of Singularly Perturbed Mechanical Systems*. Lecture Notes in Mathematics, vol. 1687. Berlin: Springer.

Bornemann, F. A. & Schütte, C. (1995) *A Mathematical Approach To Smoothed Molecular Dynamics: Correcting Potentials for Freezing Bond Angles*, Berlin: Konrad-Zuse-Zentrum für Informationstechnik Berlin.

Bornemann, F. A. & Schütte, C. (1997) Homogenization of Hamiltonian systems with a strong constraining potential. *Phys. D*, **102**, 57–77.

Bou-Rabee, N. & Marsden, J. E. (2009) Hamilton–Pontryagin integrators on Lie groups part I: introduction and structure-preserving properties. *Found. Comput. Math.*, **9**, 197–219.

Bou-Rabee, N. & Owhadi, H. (2010) Long-run accuracy of variational integrators in the stochastic context. *SIAM J. Numer. Anal.*, **48**, 278–297.

Channell, P. J. & Scovel, C. (1990) Symplectic integration of Hamiltonian systems. *Nonlinearity*, **3**, 231.

Chiba, F. & Kako, T. (2002) Newmark's method and discrete energy applied to resistive mhd equation. *Vietnam J. Math.*, **30**, 501–520.

Erlicher, S., Bonaventura, L. & Bursi, O. S. (2002) The analysis of the generalized α method for non-linear dynamic problems. *Comput. Mech.*, **28**, 83–104.

Faou, E. & Grebert, B. (2011) Hamiltonian interpolation of splitting approximations for nonlinear PDEs. *Found. Comput. Math.*, **11**, 381–415.

Filbet, F. & Jin, S. (2010) A class of asymptotic preserving schemes for kinetic equations and related problems with stiff sources. *J. Comput. Phys.*, **229**, 7625–7648.

Fixman, M. (1974) Classical statistical mechanics of constraints: a theorem and application to polymers. *Proc. Natl Acad. Sci. USA*, **71–8**, 3050–3053.

García-Archilla, B., Sanz-Serna, J. M. & Skeel, R. D. (1999) Long-time-step methods for oscillatory differential equations. *SIAM J. Sci. Comput.*, **20**, 930–963.

Greengard, L. F. & Rokhlin, V. (1987) A fast algorithm for particle simulations. *J. Comput. Phys.*, **73**, 325–348.

Hairer, E., Lubich, C. & Wanner, G. (2006) *Geometric Numerical Integration: Structure-Preserving Algorithms for Ordinary Differential Equations*, 2nd edn. Berlin: Springer.

Hairer, E. & Wanner, G. (1996) *Solving Ordinary Differential Equations II*, 2nd edn. Berlin: Springer.

Hartmann, C. (2008) An ergodic sampling scheme for constrained Hamiltonian systems with applications to molecular dynamics. *J. Stat. Phys.*, **130**, 687–711.

Hess, B., Bekker, H., Berendsen, H. J. C. & Fraaije, J. G. E. M. (1997) LINCS: a linear constraint solver for molecular simulations. *J. Comput. Chem.*, **18**, 1463–1472.

Hesthaven, J. S., Gottlieb, S. & Gottlieb, D. (2007) *Spectral Methods for Time-Dependent Problems*. Cambridge Monographs on Applied and Computational Mathematics, vol. 21. UK: Cambridge University Press.

Holm, D. D., Marsden, J. E. & Ratiu, T. S. (1998) The Euler–Poincaré equations and semidirect products with applications to continuum theories. *Adv. Math.*, **137**, 1–81.

Hughes, T. J. R. (1977) A note on the stability of newmark's algorithm in nonlinear structural dynamics. *Int. J. Numer. Methods Eng.*, **11**, 383–386.

Iserles, A. (2001) On Cayley-transform methods for the discretization of Lie-group equations. *Found. Comput. Math.*, **1**, 129–160.

Iserles, A., Munthe-Kaas, H. Z., Nørsett, S. P. & Zanna, A. (2000) Lie-group methods. *Acta Numer.*, **9**, 215–365.

Jain, A., Vaidehi, N. & Rodriguez, G. (1993) A fast recursive algorithm for molecular dynamics simulation. *J. Comput. Phys.*, **106**, 258–268.

Jorgensen, W. L., Chandrasekhar, J., Madura, J. D., Impey, R. W. & Klein, M. L. (1983) Comparison of simple potential functions for simulating liquid water. *J. Chem. Phys.*, **79**, 926.

Junge, O. & Ober-Bloebaum, S. (2005) Optimal reconfiguration of formation flying satellites. *Proceedings of 44th IEEE Conference on Decision and Control and the European Control Conference 2005*, IEEE, New York, pp. 66–71.

Kane, C., Marsden, J. E., Ortiz, M. & West, M. (2000) Variational integrators and the Newmark algorithm for conservative and dissipative mechanical systems. *Int. J. Numer. Methods Eng.*, **49**, 1295–1325.

Kevorkian, J. & Cole, J. D. (1996) *Multiple Scale and Singular Perturbation Methods*. Applied Mathematical Sciences, vol. 114. New York: Springer.

Kobilarov, M., Crane, K. & Desbrun, M. (2009) Lie group integrators for animation and control of vehicles. *ACM Trans. Graph.*, **28**, 16.

Koon, W., Owhadi, H., Tao, M. & Yanao, T. (2013) Control of a model of DNA division via parametric resonance. *Chaos*, **23**, 013117.

Kräutler, V., van Gunsteren, W. F. & Hnenberger, P. H. (2001) A fast SHAKE algorithm to solve distance constraint equations for small molecules in molecular dynamics simulations. *J. Comput. Chem.*, **22**, 501–508.

Kuhl, D. & Ramm, E. (1996) Constraint energy momentum algorithm and its application to non-linear dynamics of shells. *Comput. Methods Appl. Mech. Eng.*, **136**, 293–315.

Lee, T., Leok, M. & McClamroch, N. H. (2007) Lie group variational integrators for the full body problem. *Comput. Methods Appl. Mech. Eng.*, **196**, 2907–2924.

Leimkuhler, B. & Reich, S. (2004) *Simulating Hamiltonian Dynamics*. Cambridge Monographs on Applied and Computational Mathematics, vol. 14. Cambridge: Cambridge University Press.

Lelièvre, T., Rousset, M. & Stoltz, G. (2012) Langevin dynamics with constraints and computation of free energy differences. *Math. Comput.*, **81**, 2071–2125.

Li, T., Abdulle, A. & E, W. (2008) Effectiveness of implicit methods for stiff stochastic differential equations. *Commun. Comput. Phys.*, **3**, 295–307.

Marsden, J. E. & Ratiu, T. S. (2010) *Introduction to Mechanics and Symmetry*, 2nd edn. Berlin: Springer.

Marsden, J. E. & West, M. (2001) Discrete mechanics and variational integrators. *Acta Numer.*, **10**, 357–514.
McLachlan, R. I. & Atela, P. (1992) The accuracy of symplectic integrators. *Nonlinearity*, **5**, 541.
Mezić, I. (2006) On the dynamics of molecular conformation. *Proc. Natl Acad. Sci.*, **103**, 7542–7547.
Miyamoto, S. & Kollman, P. A. (1992) Settle: an analytical version of the SHAKE and RATTLE algorithm for rigid water models. *J. Comput. Chem.*, **13**, 952–962.
Neri, F. (1988) Lie algebras and canonical integration. *Technical Report*. Department of Physics, University of Maryland.
Newmark, N. M. (1959) A method of computation for structural dynamics. *Proc. ASCE*, **85**, 67–94.
Perchak, D., Skolnick, J. & Yaris, R. (1985) Dynamics of rigid and flexible constraints for polymers. Effect of the Fixman potential. *Macromolecules*, **18**, 519–525.
Platt, J. C. & Barr, A. H. (1988) Constraints methods for flexible models. *SIGGRAPH Comput. Graph.*, **22**, 279–288.
Reich, S. (1995) Smoothed dynamics of highly oscillatory Hamiltonian systems. *Phys. D*, **89**, 28–42.
Richter, P. H. & Scholz, H.-J. (1984) *Stochastic Phenomena and Chaotic Behaviour in Complex Systems*. Berlin: Springer.
Rubin, H. & Ungar, P. (1957) Motion under a strong constraining force. *Commun. Pure Appl. Math.*, **10**, 65–87.
Ryckaert, J.-P., Ciccotti, G. & Berendsen, H. J. C. (1977) Numerical integration of the cartesian equations of motion of a system with constraints: molecular dynamics of n-alkanes. *J. Comput. Phys.*, **23**, 327–341.
Sanz-Serna, J. M. (2008) Mollified impulse methods for highly oscillatory differential equations. *SIAM J. Numer. Anal.*, **46**, 1040–1059.
Schlick, T. (2010) *Molecular Modeling and Simulation*, 2nd edn. Berlin: Springer.
Schütte, C. & Bornemann, F. A. (1997) Homogenization approach to smoothed molecular dynamics. *Nonlinear Anal. Theory Methods Appl.*, **30**, 1805–1814.
Shatah, J. & Zeng, C. (2002) Periodic solutions for Hamiltonian systems under strong constraining forces. *J. Differential Equations*, **186**, 572–585.
Skeel, R. D. & Srinivas, K. (2000) Nonlinear stability analysis of area-preserving integrators. *SIAM J. Numer. Anal.*, **38**, 129–148.
Skeel, R. D., Zhang, G. & Schlick, T. (1997) A family of symplectic integrators: stability, accuracy, and molecular dynamics applications. *SIAM J. Sci. Comput.*, **18**, 203–222.
Takens, F. (1980) Motion under the influence of a strong constraining force. *Global Theory of Dynamical Systems*. Berlin: Springer, pp. 425–445.
Tao, M., Owhadi, H. & Marsden, J. E. (2010) Nonintrusive and structure preserving multiscale integration of stiff ODEs, SDEs and Hamiltonian systems with hidden slow dynamics via flow averaging. *Multiscale Model. Simul.*, **8**, 1269–1324.
Tao, M., Owhadi, H. & Marsden, J. E. (2011) From efficient symplectic exponentiation of matrices to symplectic integration of high-dimensional Hamiltonian systems with slowly varying quadratic stiff potentials. *Appl. Math. Res. Express*, **2011**, 242–280.
Terzopoulos, D., Platt, J., Barr, A. & Fleischer, K. (1987) Elastically deformable models. *SIGGRAPH Comput. Graph.*, **21**, 205–214.
Toit, P. D., Mezić, I. & Marsden, J. (2009) Coupled oscillator models with no scale separation. *Phys. D*, **238**, 490–501.
van der Spoel, D., van Maaren, P. J. & Berendsen, H. J. C. (1998) A systematic study of water models for molecular simulation: derivation of water models optimized for use with a reaction field. *J. Chem. Phys.*, **108**, 10220.
Vanden-Eijnden, E. & Ciccotti, G. (2006) Second-order integrators for Langevin equations with holonomic constraints. *Chem. Phys. Lett.*, **429**, 310–316.
Wendlandt, J. M. & Marsden, J. E. (1997) Mechanical integrators derived from a discrete variational principle. *Phys. D*, **106**, 223–246.

Witkin, A., Fleischer, K. & Barr, A. (1987) Energy constraints on parameterized models. *SIGGRAPH Comput. Graph.*, **21**, 225–232.
Wood, W. L. & Oduor, M. E. (1988) Stability properties of some algorithms for the solution of nonlinear dynamic vibration equations. *Commun. Appl. Numer. Methods*, **4**, 205–212.
Yoshida, H. (1990) Construction of higher order symplectic integrators. *Phys. Lett. A*, **150**, 262–268.
Zhang, M. & Skeel, R. D. (1997) Cheap implicit symplectic integrators. *Appl. Numer. Math.*, **25**, 297–302.

Appendix

Lemma A.1 Consider (1.7). If V is bounded from below, then there is a constant C, such that $\|g(q^\omega(s))\| \leqslant C/\omega$ for all s. Moreover, if $V(q)$ diverges to infinity as $|q| \to \infty$, then there is a constant $\tilde{C}$ such that $\|q^\omega(s)\| \leqslant \tilde{C}$.

Proof. Note that the energy $[\dot{q}^\omega]^{\mathrm{T}} M \dot{q}^\omega/2 + V(q^\omega) + \omega^2 g(q^\omega)^{\mathrm{T}} g(q^\omega)$ in the penalized system (1.7) is conserved and determined by the initial condition. Therefore, $V(\cdot)$ being bounded from below and $g^{\mathrm{T}} g \geqslant 0$ imply that $\omega^2 g(q^\omega)^{\mathrm{T}} g(q^\omega) = \mathcal{O}(1)$. Hence, $g(q^\omega(s)) = \mathcal{O}(1/\omega)$.

By a similar energy argument, since $[\dot{q}^\omega]^{\mathrm{T}} M \dot{q}^\omega/2 \geqslant 0$ and $g(q^\omega)^{\mathrm{T}} g(q^\omega) \geqslant 0$, $V(q^\omega)$ is bounded from above too, which implies that q^ω remains bounded. □

Lemma A.2 Consider the solution to a conserved mechanical system

$$\begin{cases} \ddot{x}^\omega = f_1(x^\omega, y^\omega), \\ \ddot{y}^\omega = f_2(x^\omega, y^\omega) - \omega^2 g(y^\omega)^{\mathrm{T}} \nabla g(y^\omega), \end{cases} \tag{A.1}$$

where x^ω and y^ω are vectors, and $x^\omega(0) = x_0$, $\dot{x}^\omega(0) = \dot{x}_0$, $y^\omega(0) = y_0$, $\dot{y}^\omega(0) = \dot{y}_0$. Suppose that f_1, f_2 and ∇g are C^1 with bounded derivatives, x^ω and y^ω are bounded, $g(y_0) = 0$ and $(\mathrm{d}/\mathrm{d}t) g(y_0) = 0$, and $g(\cdot)$ has a non-degenerate Jacobian in a neighbourhood of y_0; then

$$\lambda(t) := -\lim_{T \to 0} \lim_{\omega \to \infty} \frac{1}{T} \int_t^{t+T} \omega^2 g(y^\omega(s))\, \mathrm{d}s \tag{A.2}$$

exists and is finite. Denote by $x(t)$, $y(t)$ the solution to

$$\begin{cases} \ddot{x} = f_1(x, y), \\ \ddot{y} = f_2(x, y) + \lambda^{\mathrm{T}} \nabla g(y), \\ g(y) = 0, \end{cases} \tag{A.3}$$

with the same initial conditions $x_0, \dot{x}_0, y_0, \dot{y}_0$; then, as $\omega \to \infty$,

$$\begin{cases} x^\omega \to x, \\ y^\omega \xrightarrow{F} y, \\ g(y^\omega) \to 0. \end{cases} \tag{A.4}$$

Proof. We employ the multiscale averaging framework described in Tao *et al.* (2010) to demonstrate the convergence. Here, x^ω is a slow variable and its evolution corresponds to the constrained dynamics; y^ω is a fast variable corresponding to a fluctuating deviation from the constraint manifold at a characteristic timescale of $\mathcal{O}(1/\omega)$, and it lies in the normal bundle of the constraint manifold.

First, consider the linear constraint case in which $g(y) = Cy^{\mathrm{T}}$ for some nonsingular C (the affine case can be similarly treated by shifting y). We see that y dynamics is governed by

$$\ddot{y}^{\omega} = f_2(x^{\omega}, y^{\omega}) - \omega^2 y^{\omega} C^{\mathrm{T}} C. \tag{A.5}$$

This is a forced harmonic oscillator, and its solution can be written as

$$y^{\omega}(t) = \int_0^t f_2(x^{\omega}(s), y^{\omega}(s)) \sin(\omega \tilde{C} s) \tilde{C}^{-1} / \omega \, \mathrm{d}s, \tag{A.6}$$

where $\tilde{C} = \sqrt{C^{\mathrm{T}} C}$ is the well-defined matrix square root, and matrix sin is defined either by Taylor expansion or diagonalization. Note that there is no propagation of the initial condition because $y^{\omega}(0) = 0$.

It can be shown from (A.6) (for instance, by Tao *et al.*, 2011, Lemma 3.8; the idea is that an addition $1/\omega$ comes from the sin due to integration by parts) that $y^{\omega}(t)$ is $\mathcal{O}(\omega^{-2})$ at least up to $t = o(1)$, and y^{ω} is asymptotically periodic (because (A.5) is asymptotically linear), and hence locally ergodic on the energy shell (with Dirac ergodic measure).

Since y^{ω} is locally ergodic on the energy shell, (A.2) well defines λ, and Tao *et al.* (2010, Theorem 1.2) guarantees that the effective equation for (A.5) is

$$\ddot{y} = f_2(x^{\omega}, y) + \lambda^{\mathrm{T}} C, \tag{A.7}$$

in the sense that $y^{\omega} \xrightarrow{F} y$ and $x^{\omega} \to x$. Note that the convergence on x is in the strong sense, i.e., $\lim_{\omega \to \infty} x^{\omega}(t) \to x(t)$ for all bounded $t > 0$. This is because x is purely slow, for which case, F-convergence implies strong convergence.

Now, consider a fully nonlinear $g(\cdot)$ with a nondegenerate Jacobian. Lemma A.1 gives that $g(y^{\omega}) = \mathcal{O}(1/\omega)$. Since y^{ω} is by assumption bounded, inverting g leads to $y^{\omega} - y_0 = \mathcal{O}(1/\omega)$. Consequently, the dynamics of y^{ω} approaches that of a forced oscillator (with equilibrium at y_0) at an $\mathcal{O}(1/\omega)$ timescale, because $g(\cdot)$ is approximated by its first-order Taylor expansion:

$$\begin{aligned}
\ddot{y^{\omega}} &= f_2(x^{\omega}, y^{\omega}) - \omega^2 g(y^{\omega})^{\mathrm{T}} \nabla g(y^{\omega}) \\
&= f_2(x^{\omega}, y^{\omega}) - \omega^2 \left(\nabla g(y_0)(y^{\omega} - y_0)^{\mathrm{T}} + \mathcal{O}(\omega^{-2}) \right)^{\mathrm{T}} \left(\nabla g(y_0) + \mathrm{Hess}\, g(y_0)(y^{\omega} - y_0)^{\mathrm{T}} + \mathcal{O}(\omega^{-2}) \right) \\
&= f_2(x^{\omega}, y^{\omega}) - \omega^2 (y^{\omega} - y_0) \nabla g(y_0)^{\mathrm{T}} \nabla g(y_0) + \mathcal{O}(1),
\end{aligned}$$

where nonlinearity $f_2 + \mathcal{O}(1)$ again manifests as a slow force, which is dominated by the linear term that leads to asymptotically periodic oscillations. Hence, similar to the linear case, y^{ω} is locally ergodic on the energy shell, the Lagrange multiplier λ is well-defined and the solution x^{ω}, y^{ω} F-converges to the effective solution x, y. □

Sketch of the proof of Theorem 1.3. (Figure A1 illustrates the notation used in the proof to help understand the geometry.) Since $g(q^{\omega})$ is at most $\mathcal{O}(1/\omega)$ (Lemma A.1), q^{ω} is close to the constraint manifold

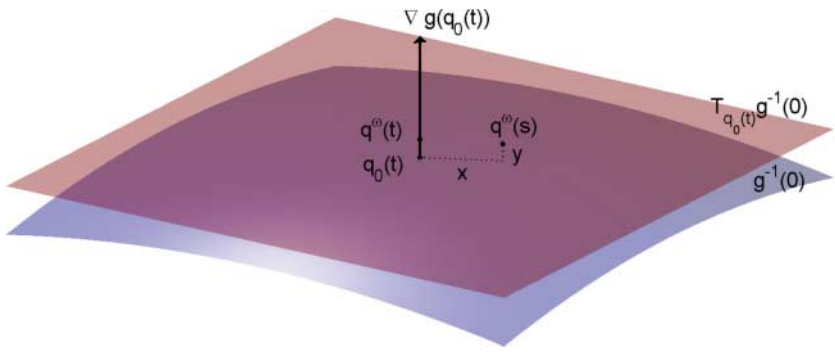

FIG. A1. Multiscale geometry of penalized constrained dynamics – x and y are slow and fast.

$g^{-1}(0)$ in the sense that if we define, for all t,

$$q_0(t) := \min_{q \in g^{-1}(0)} \|q - q^\omega(t)\| \tag{A.8}$$

then $q^\omega(t) - q_0(t) = \mathcal{O}(1/\omega)$. Indeed, given that ∇g has the maximum rank, $\nabla g(q_0(t))$ spans the normal section (i.e., the subspace perpendicular to the tangent subspace) of the constraint manifold, in which $q^\omega(t) - q_0(t)$ also lies. Moreover, g restricted to each normal section is an isomorphism, and both the restricted map and its inverse have bounded norms due to the boundedness of q^ω (i.e., compactness of the solution space)—this is why $g(q^\omega) = \mathcal{O}(1/\omega)$ implies $q^\omega(t) - q_0(t) = \mathcal{O}(1/\omega)$.

The idea is that since q^ω is close enough, the constraint manifold can be locally viewed as a flat subspace, and F-convergence for this case has been proved in Lemma A.2. More precisely, there exists a linear isomorphism $A_{q_0(t)}$, such that

$$A_{q_0(t)}(q^\omega(t) - q_0(t)) = \begin{bmatrix} 0 \\ y \end{bmatrix}, \tag{A.9}$$

where y is a vector with codimension of $g^{-1}(0)$ and 0 is a null vector.

For $q^\omega(s)$ with $s - t = \mathcal{O}(1/\omega)$, we will have a full-dimensional representation:

$$A_{q_0(t)}(q^\omega(s) - q_0(t)) = \begin{bmatrix} x \\ y \end{bmatrix}, \tag{A.10}$$

and x and y will, respectively, be the slow and fast variables, representing the constrained dynamics and fluctuations away from the constraint manifold (analogous to Lemma A.2). This is because

$$\begin{aligned} \frac{\mathrm{d}^2}{\mathrm{d}s^2} \begin{bmatrix} x \\ y \end{bmatrix} &= A_{q_0(t)}(-\nabla V(q^\omega(s)) - \omega^2 g(q^\omega(s)) \nabla g(q^\omega(s))) \\ &= \begin{bmatrix} f_1(x,y) \\ f_2(x,y) \end{bmatrix} + \begin{bmatrix} \mathcal{O}(1) \\ -\omega^2 \tilde{g}(y) \nabla \tilde{g}(y) + \mathcal{O}(1) \end{bmatrix}, \end{aligned} \tag{A.11}$$

where f_1 and f_2 are defined as $A_{q_0(t)}(-\nabla V(q^\omega(s)))$. The $\mathcal{O}(1)$ in the first row of the right-hand side of (A.11) is because $A_{q_0(t)}$ rotates the normal section to the y-direction, i.e.,

$$A_{q_0(t)}\nabla g(q^\omega(s)) = A_{q_0(t)}(\nabla g(q_0) + \mathcal{O}(1/\omega)) = \begin{bmatrix} 0 \\ * \end{bmatrix} + \mathcal{O}(1/\omega), \tag{A.12}$$

where $*$ is some nonzero expression, and certainly $\mathcal{O}(1/\omega) = \mathcal{O}(1)$.

The $\mathcal{O}(1)$ in the second row of the right-hand side of (A.11) can also be intuitively obtained by using an analogous geometric argument, together with Taylor expansion.

Since (A.11) corresponds to the locally flat system (A.1), Lemma (A.2) proved the existence of an equivalent Lagrange multiplier as well as the F-convergence towards it. Moreover, (A.11) and the global dynamics near the curved constraint manifold (1.7) is linked via a coordinate transformation $q^\omega \mapsto A_{q_0}(q^\omega - q_0)$, which, naturally, is slowly varying as q_0 changes. Since averaging via F-convergence (Tao *et al.*, 2010, Theorem 1.2) still works if the slow and fast variables are images of the original variable under a slowly varying diffeomorphism, the global dynamics (1.7) is F-convergent to a solution of (1.9). Note that $g(q(t)) = 0$ in (1.9) is automatically satisfied, because $\lim_{\omega\to\infty} g(q^\omega(t)) = 0$.

Finally, the solution to (1.9) is also the solution to (1.6). This is by the existence and uniqueness of the solution to differential algebraic equations with initial conditions.

(Only main lines of the proof are provided; details are similar to analysis in Tao *et al.*, 2010, 2011.) □

REMARK A.3 The above proofs show that $g(q^\omega(s))$ is not only $\mathcal{O}(\omega^{-1})$, but also $\mathcal{O}(\omega^{-2})$.